UNIVERSITI
MALAYSIA
KELANTAN

Effect of Calcium Copper Titanate ($CaCu_3Ti_4O_{12}$)/ Barium Titanate ($BaTiO_3$) Composition in Electrical and Microstructural Properties

MUHAMAD AFIF ZAAFARANI BIN MUHAMAD AIDI
J20A0673

A thesis submitted in fulfilment of the requirements for the degree of Bachelor of Applied Science (Materials Technology) with Honours

FACULTY OF BIOENGINEERING AND TECHNOLOGY

UMK

2024

DECLARATION

I declare that this thesis entitled "EFFECT OF CALCIUM COPPER TITANATE ($CaCu_3Ti_4O_{12}$)/BARIUM TITANATE ($BaTiO_3$) COMPOSITION IN ELECTRICAL AND MICROSTRUCTURAL PROPERTIES" is the result of my own research except as cited in the reference. The thesis has not been accepted for any degree and is not concurrently submitted in candidature of any other degree.

_____

Signature:

Name: Muhamad Afif Zaafarani Bin Muhamad Aidi

No.matric: J20A0673

Date:

_____

Signature:

Name: Associate Prof. Dr Muhammad Azwadi Bin Sulaiman

Stamp:

Date:

ACKNOWLEDGEMENT

Bismillahirrahmanirrahim. In the name of Allah, The Most Beneficent and The Most Merciful. First and foremost, I want to thank Allah SWT for providing me with the health and strength I needed to finish the final project. My sincere gratitude also goes out to the Faculty of Biotechnology and Engineering at Universiti Malaysia Kelantan and particularly to Associate Prof. Dr. Muhammad Azwadi bin Sulaiman, who had been a very helpful supervisor who guided, supervises, and gave me many insightful advice over the course of the project.

In addition, I would like to thank my UMK friends Aidi Adam bin Mohd Raof, Nurul Syazlin Binti Aminuddin, Nur Zaimah Atikah Binti Mohd Zain and all the friend for their unwavering support and assistance in helping me finish this project. I would also like to thank to lab assistant, Ts. Pn Hanisah Izzati and En.Qamal who has assisted me throughout the experiment.

Lastly, I would like to express my sincere gratitude to my parents, Mr. Mazlan bin Md Hussain and Mrs. Yusmawati binti Che Yahya, for their support throughout this project both in financially, morally and for their understanding and unwavering love.

Effect of Calcium Copper Titanate ($CaCu_3Ti_4O_{12}$)/ Barium Titanate ($BaTiO_3$) Composition in Electrical and Microstructural Properties

ABSTRACT

Barium Titanate (BT) and Calcium Copper Titanate (CCTO) are renowned for their high dielectric properties, and they have been extensively researched for the miniaturization of microelectronic devices. Integrating CCTO's high dielectric constant property with BT's low loss as a composite could leverage the benefits of both compounds. This research explores the electrical and microstructural behavior of BT and CCTO in their composite form, synthesized via the solid-state reaction method. The composite mixture was formulated according to $BaTiO_3.xCaCu_3Ti_4O_{12}$, where x = 0.2, 0.5, 1, 1.2, and 1.5 mol%. A semi-quantitative analysis confirmed the composition, with minor variations potentially arising from milling factors. Notably, the milling process led to the formation of oxygen vacancies, as observed from the TGA/DSC analysis. Next, sintered pallets samples were treated with furnace for 1050℃ in 10 hours. Samples were characterised for electrical, microstructural and morphology properties. The microstructure of the composite also showed the crystal of CCTO immersed in the BT with good surface contact and the surface morphology show that has many pores and agglomeration of CCTO particles, which reduce its mechanical strength. While, for both density and porosity, the density of CCTO/BT which is 0.2mol% pallet at 4.21g/cm^3 and the lowest is 1.2mol% pallet at 2.66g/cm^3 meanwhile for porosity 0.5mol% has the lowest porosity. For electrical properties, it shows an increasing CCTO/BT content can improve the dielectric constant from between 7.54 and 50.5 at 10 MHz and dielectric loss is decreasing from 6.1 to 1.0 at 10 MHz. In conclusion, all the testing that throughout, the most excellent composition that exhibits excellent properties is 1.2mol% of CCTO/BT.

Keywords: Calcium Copper Titanate, Barium Titanate, Composite Composition, Morphology, Microstructural, Electrical

Kesan Komposisi Kalsium Kupro Titanat ($CaCu_3Ti_4O_{12}$)/ Barium Titanat ($BaTiO_3$) terhadap Sifat Elektrik dan Mikrostruktur

ABSTRAK

Barium Titanat (BT) dan Kalsium Kupro Titanat (CCTO) terkenal dengan sifat dielektrik yang tinggi, dan mereka telah banyak diselidiki untuk pengecilan peranti mikroelektronik. Mengintegrasikan sifat konstanta dielektrik tinggi CCTO dengan kehilangan rendah BT sebagai komposit dapat memanfaatkan manfaat kedua senyawa tersebut. Kajian ini meneroka tingkah laku elektrik dan mikrostruktur BT dan CCTO dalam bentuk komposit mereka, disintesis melalui kaedah tindak balas keadaan pepejal. Campuran komposit diformulasikan mengikut $BaTiO_3$.$x CaCu_3Ti_4O_{12}$, di mana x = 0.2, 0.5, 1, 1.2, dan 1.5 mol%. Analisis semi-kuantitatif mengesahkan komposisi, dengan variasi kecil mungkin timbul dari faktor penggilingan. Secara khusus, proses penggilingan mengakibatkan pembentukan kedudukan vakum oksigen, seperti yang diperhatikan daripada analisis TGA/DSC. Seterusnya, sampel palet disinter dengan diperlakukan dengan dapur selama 1050℃ dalam masa 10 jam. Sampel dikarakterisasikan untuk sifat-sifat elektrik, mikrostruktur dan morfologi. Mikrostruktur komposit juga menunjukkan kristal CCTO terbenam dalam BT dengan kontak permukaan yang baik dan morfologi permukaan menunjukkan terdapat banyak liang dan penggumpalan zarah CCTO, yang mengurangkan kekuatan mekanikalnya. Sementara itu, untuk kepadatan dan porositi, kepadatan CCTO/BT yang tertinggi adalah pada palet 0.2mol% pada 4.21g/cm^3 dan yang terendah adalah pada palet 1.2mol% pada 2.66g/cm^3, sementara untuk porositi, 0.5mol% mempunyai porositi terendah. Untuk sifat-sifat elektrik, ia menunjukkan peningkatan kandungan CCTO/BT dapat meningkatkan konstanta dielektrik dari antara 7.54 dan 50.5 pada 10 MHz dan kehilangan dielektrik berkurangan dari 6.1 hingga 1.0 pada 10 MHz. Kesimpulannya, setelah semua ujian yang dijalankan, komposisi terbaik yang menunjukkan sifat-sifat yang cemerlang adalah 1.2mol% CCTO/BT.

Kata kunci: Kalsium Kupro Titanat, Barium Titanat, Komposisi Komposit, Morfologi, Mikrostruktur, Elektrik

TABLE OF CONTENT

LIST OF TABLES

LIST OF FIGURES

LIST OF ABBREVIATIONS

$BaTiO_3$/BT	Barium Titanate
CCTO	Calcium Cooper Titanate
CuO	Cooper Oxide
$CaCO_3$	Calcium Carbonate
TiO_3	Titanium Oxide
CO_2	Carbon Dioxide
XRD	X-ray Diffraction
TGA	Thermogravimetric Analysis
EDX	Energy Dispersive X-ray
SEM	Scanning Electron Microscope
DSC	Differential Calorimetry Analysis

LIST OF SYMBOLS

℃	Degree Celsius
%	Percentage
M	Molar
ml	Millimetre
g	Gram
MHz	Mega Heartz
kHz	Kilo Heartz

CHAPTER 1

INTRODUCTION

1.1 Background of Study

Since technology has continued to advance, numerous types of advanced ceramics have been created for a variety of industrial applications. Advanced ceramics are materials that have had their chemical composition altered and internal structure to achieve the desired ceramic properties, such as superior mechanical properties, resistance to oxidation or corrosion, thermal, electrical, optical, or magnetic properties to meet industry demands. Research on the use of advanced ceramics in electronic devices, such as capacitors, insulators, substrates, integrated circuit packages, piezoelectric, magnets, and superconductors, is among the most widely pursued fields of study (Glazer, 1972).

According to Glazer, (1972), a material with a high dielectric constant can store a lot of energy, and vice versa, since a material with a low dielectric constant cannot store energy when an electric field is present. Dielectric materials are those that can store energy when an electric field is present. $CaCu_3Ti_4O_{12}$, or calcium copper titanate (CCTO) with a cubic perovskite structure that is body centred. In is one of the most well-liked ceramics in scientific circles because of its high dielectric constant, which is approximately 100,000 for bulk material at room temperature (Ab Rahman et al., 2015) with a good temperature stability in the range from 100 K-600 K (Subramanian et al., 2000)

According to Ab Rahman et al., (2015), due to its large dielectric constant and ability to store large amounts of energy, these characteristics make CCTO a potential candidate for use in microelectronic devices. As a result, small-sized devices with large energy storage capacities can be produced. Although CCTO have a very high dielectric constant, this property also has a high dielectric loss (>0.05), which is a drawback (Jumpatam et al., 2014). Some techniques, such as doping, have been developed to address the issue because of the high value of dielectric loss. To enhance a material's properties, a small number of impurities with the same atomic size are added to it through the process of doping.

In this case, Barium Titanate ($BaTiO_3$, BT) has been choosing as material due to ability to enhance the electrical properties of CCTO by increasing the dielectric permittivity and decreasing the dielectric loss (Tewatia et al., 2020). The addition of barium titanate can aid in lowering the composite material's dielectric loss in addition to raising the dielectric permittivity. Dielectric loss is a measurement of the amount of energy lost as heat when an alternating electric field is applied. BT and CCTO can be combined to create a composite material with lower dielectric loss and higher electrical efficiency.

1.2 Problem Statement

The problem statement for studying the effect BT/CCTO composition on the electrical and microstructural properties arises from the need to develop composite materials with improved electrical properties for various applications such as energy storage, capacitors, and electronic devices. Due to its special electrical properties, barium titanate, which has a perovskite crystal structure, is frequently used in a variety of electronic applications. Ferroelectric properties of BT make it useful in the creation of electronic devices like capacitors, sensors, and actuators (Pant et al., 2006). It is suitable for applications requiring high capacitance because of its high dielectric constant. Electronic circuits frequently use barium titanate capacitors. Due to its piezoelectric properties, BT can produce an electric charge when mechanical stress is applied, or vice versa. This characteristic is used in microphones, ultrasound equipment, and transducers. Due to their frequent relatively high dielectric loss, CCTO ceramics may not be suitable for all electronic devices. Dielectric loss can be influenced by microstructural elements like grain boundaries, porosity, and secondary phases (Zhang et al., 2019). Thus, combining BT and CCTO in a composite material could result in a material with improved electrical properties compared to the individual components. The microstructure and morphology of the composite material can significantly influence its electrical properties, such as dielectric constant, tunability, loss and breakdown strength. Therefore, understanding the relationship between the composition, microstructure, and electrical properties of BT-CCTO composites is crucial for developing composite materials with optimized properties. The effect of the composition and microstructure of BT-CCTO composites on their electrical properties are also not well understood.

1.3 Objectives

There are three objectives to be achieved in this research as stated below:

I. To synthesize composite with different composition $BaTiO_3$ and CCTO using solid-state method.

II. To characterize the electrical properties and microstructural of the composite materials.

III. To establish the relationship between the composition, electrical properties, and microstructure of the composite material.

1.4 Scope of Study

The scope of this study is how to synthesize different composition BT/CCTO using solid-state method. The BT-CCTO can be characterize their electrical properties and microstructural of composite using X-ray diffraction (XRD), Scanning Electron Microscope (SEM) and LCR analyzer. Finally, the relationship of BT-CCTO between the composition, electrical properties and microstructure of the composite material will be getting.

1.5 Significances of Study

The result and discovery from this study are hoped that can understanding the relationship between the Barium Titanate ($BaTiO_3$)/Calcium Copper Titanate (CCTO) composite's composition and properties. It can help individuals create new materials with improved electrical and microstructural properties. Analysis of the BT/CCTO microstructure, including density and porosity had been part of the study. Microscopy,

X-ray diffraction, and thermogravimetric analysis are examples of microstructural characterization techniques that can provide detailed information about the arrangement and quality of the crystalline structure. It also can evaluate $BaTiO_3$ and CCTO's suitability for applications by contrasting their electrical characteristics and microstructure. $BaTiO_3$ might be preferred, for instance, if high dielectric permittivity is needed, whereas CCTO might work well in applications that call for lower dielectric loss and higher electrical conductivity.

CHAPTER 2

LITERATURE REVIEW

2.1 Ceramic

The properties of ceramics, an inorganic material type, are derived from the interaction between their metallic and non-metallic elements. The most versatile material class is ceramics. Because its bonds are a combination of covalent and ionic interactions of differing strengths, it is malleable. Numerous aspects of ceramic materials, including bonding, are determined by these attributes, which include relatively high fusion temperatures, high modulus, high wear power, poor thermal properties, high hardness, and fragilities mixed with tenacities, and low ductility. Because of the chemical links that hold them together, they act as effective electrical insulators despite lacking conduction electrons(Eliche-quesada & Pérez-villarejo, 2019).

Advanced ceramics are fabricated from synthetic raw materials that have been subjected to intensive chemical processing to achieve a high degree of purity and improve upon their physical qualities. Therefore, sophisticated, and forward-thinking methods are used in their production. Applications in magnetism, ferroelectricity, piezoelectricity, and superconductivity are found in a broad variety of ceramics, including carbides, nitrides, borides, pure oxides, and others.

2.2 Composite

The term "composite" refers to a mixture of two or more types of materials, one of which serves as a matrix and the other as reinforcement. However, it can also be described as a substance that has a chemically or physically distinct phase dispersed within a continuous phase. The reinforcement material may be different in size and shape. The three types of composite materials are generally known as polymer matrix composites (PMC), metal matrix composites (MMC), and ceramic matrix composites (CMC) (Egbo, 2021).

2.3 Barium Titanate ($BaTiO_3$)

Barium titanate ($BaTiO_3$, BT) is one of the compounds of the perovskites with the general formula ABO_3, which represents one of the secondary groups that belong to the ferroelectric materials, where (A) represents a binary or monovalent metal and (B) represents a quadrilateral or pentavalent metal (Yaseen, 2019). When BT is heated to the Curie temperature 120 ℃, a transition from the ferroelectric tetragonal phase to the paraelectric cubic phase occurs (Yaseen, 2019). Dielectric materials are used in many electrical systems and are almost always used in fields like microelectronics and high-pressure settings. BT material, which has a high dielectric constant, is frequently used in the production of capacitors. Due to the significance of this material's high dielectric properties, it has been the subject of numerous studies since the turn of the 20th century. According to Yaseen (2019), it was investigated how certain compounds added to BT as impurities would affect the material's dielectric properties.

2.4 Calcium Copper Titanite ($CaCu_3Ti_4O_{12}$)

According to Callister Jr & Rethwisch, (2018), an insulator with the potential for an electric dipole structure is called a dielectric material. Unlike metallic and semiconductor materials, insulator materials possess a larger energy bandgap. **Error! Reference source not found.Error! Reference source not found.** The perovskite structure is a particular type of crystallography found in ceramic materials with the formula ABX_3, such as $BaTiO_3$ and many more. Ti cations occupy the B-site and the X_3-site in CCTO, while Ca and Cu ions reside at the A-sites. O will then fill the X_3-site. The dielectric constant of the $ACu_3Ti_4O_{12}$ family, which was studied by (Subramanian et al., 2000)

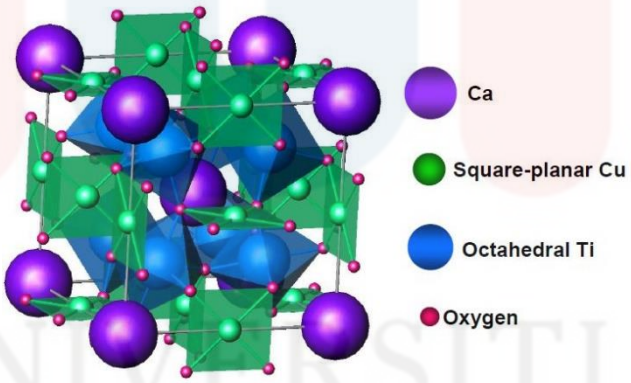

Figure 2.1: The structure of $CaCu_3Ti_4O_{12}$ shown as TiO_6 octahedral, Cu atoms bonded to four oxygen atoms, and large Ca atoms without bonds.

Source: (Subramanian et al., 2000)

2.5 Synthesis Method of Barium Titanite ($BaTiO_3$)

One of the many compounds in the large family with the general formula ABO_3 is $BaTiO_3$ perovskite composition. Different techniques can be used to make

barium titanate. The process of synthesis depends on the method used and the desired properties for the final application have a big impact on the barium titanate's composition and characteristics. Doped Barium Titanate has been extensively used in has emerged as one of the most significant ferroelectric ceramics, along with semiconductors, positive temperature coefficient resistors, ultrasonic transducers, and piezoelectric devices. It is well known that $BaTiO_3$ powders have certain characteristics and ceramics are heavily influenced by the method of synthesis and sintering regime. Different methods, such as the hydrothermal method, sol-gel processing, the oxalate route, microwave heating, a micro-emulsion process, a polymeric precursor method, ball milling, solid-state reaction, solvothermal, and various chemical routes, have been used to create $BaTiO_3$ powders (More & Topare, 2016). Solid-state reaction is the synthesis technique applied in this study.

2.5.1 Raw Materials

The basic that have in $BaTiO_3$ are Barium Carbonate ($BaCO_3$) and Titanium Oxide ($TiO_{2)}$. To find the ideal conditions for $BaTiO_3$ material preparation, $BaCO_3$ and TiO_2 compounds were mixed in a gate mortar for 12 hours at a molar ratio of 1:1. The resulting mixture and calcined at various temperatures (1100–1400 ℃) and soaking times (3–9 hr) (Yaseen, 2019). In conclusion, the decomposition of $BaTiO_3$ can be define in $BaCO_3 + TiO_2 \rightarrow BaTiO_3$ Equation 2.1.

$$BaCO_3 + TiO_2 \rightarrow BaTiO_3 \qquad \text{Equation 2.1}$$

2.5.2 Mixing and Milling Raw Material.

As a result of the destruction of agglomerates and particles from the starting precursors during mechanical activation during processing, the particles' specific surface area increases. In addition to physically reducing the size of the particles, this process also uses milling energy to start different chemical reactions among the precursors. Without an external heat source, chemical reactions take place at low temperatures while the planetary mill is operating. Additionally, high-energy milling can significantly increase the reactivity of precursors, lowering the temperature at which BT forms its phase. The microstructure of the sintered compacts has a significant impact on their dielectric properties. The characteristics of the starting powder and the chosen heating method determine the microstructure (Kumar et al., 2012).

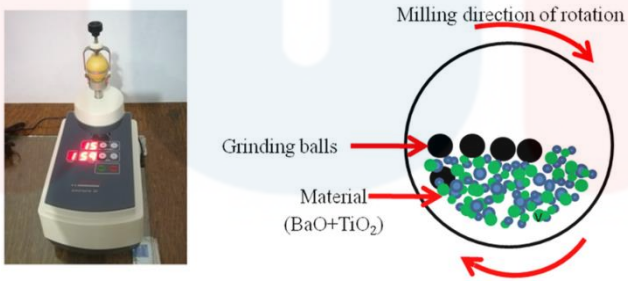

Figure 2.2: Process of mixing and milling.

Source: (Kumar et al., 2012)

2.5.3 Calcination.

During the calcination process, a high temperature had to be reached for the material or sample to eliminate volatile substances, oxidise a section of the mass, or

make them friable. After that, ion interdiffusion takes place to produce a homogenous product. Ions from nearby regions spread out until the material attains a state of balance. The sintering conditions during calcination regulate the shrinkage of the product.

According to Yaseen, (2019) study, when BT is calcined at a lower temperature (between 600℃ until 1200℃) for a brief period of time, it can lead to the secondary phase and incomplete reaction process in the sample that was examined using XRD analysis.

2.6 Synthesis Method of Calcium Copper Titanate

Solid-state reaction is the synthesis technique applied in this study. Therefore, this sub-topic will go into detail about the literature on the raw materials used and the process.

2.6.1 Raw Materials

According to Karim et al., (2017), the basic components of CCTO are powdered calcium carbonate ($CaCO_3$), titanium dioxide (TiO_2), and copper oxide (CuO). The alternative to $CaCO_3$ is calcium oxide (CaO), but CaO is an unstable substance that reacts quickly with airborne H_2O to create the stable compound Ca $(OH)_2$. This reaction also produces heat. As a result, $CaCO_3$ or Ca $(OH)_2$ will typically be chosen by other researchers. Ca $(OH)_2$. In conclusion, the decomposition of CCTO can be define in Equation 2.2, 2.3 and 2.4 below:

$$CaCO_3\ (s) \longrightarrow CaO\ (s) + CO_2\ (g) \qquad \text{Equation 2.2}$$

$$2CuO\ (s) \longrightarrow 2Cu\ (s) + O_2\ (g) \qquad \text{Equation 2.3}$$

$$TiO_2\ (s) \longrightarrow Ti\ (s) + O_2\ (g) \qquad \text{Equation 2.4}$$

2.6.2 Mixing and Milling Ceramic Raw Materials

Removing aggregates and reducing particle size are the goals of mixing and milling. For a higher quality product, it is also important to mix the powder evenly and uniformly while doing so. In their study of the structural properties of CCTO by mechanical alloying as reported by Almeida et al., (2002) draw the conclusion that the longer time spent milling and mixing the material results in the formation of nanocrystalline, which is good for nanoscale devices and applications. Alcohol was be used during mixing and milling as a dispersant, either acetone (Karim et al., 2017) or ethanol (Ahmadi pour et al., 2016)

2.6.3 Calcination

To remove volatile substances, oxidise a portion of the mass, or make them friable, the material or sample had to be heated to a high temperature during the calcination process. Ion interdiffusion then occurs to create a homogeneous final product. The ions from adjacent areas diffuse one another until the matter reaches equilibrium. The product shrinkage is controlled by the calcination conditions during sintering.

According to Karim et al., (2017) study, the secondary phase and incomplete reaction process in the sample studied using XRD analysis can result from the calcination of CCTO at a lower temperature, 900 ℃ at short of time. The homogeneous of sample should be high in order to eliminate untreated raw material.

2.7 Characterisation Technique

In this section, the basic principle and theory of suitable testing were elaborated.

2.7.1 X-Ray Diffraction

Electromagnetic radiation with high energies and brief wavelengths is referred to as X-rays. A portion of an X-ray beam that strikes a surface will scatter in all directions. A quick analytical method for determining a crystalline material's phase and providing information on the dimensions of the unit cells is X-ray diffraction (XRD). Bragg's Law can be used to explain the dimension of unit cells, as shown Figure 2.3. The relationship between the lattice vectors and the scattering vectors necessary for reflection is described by the Bragg equation.

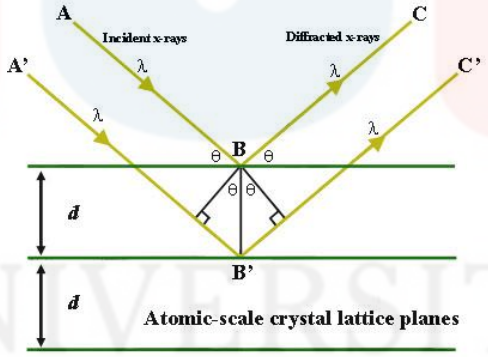

Figure 2.3: Bragg Law

Source: (Callister Jr & Rethwisch, 2018)

When the condition can satisfy Bragg's Law, the result is obtained by detecting, processing, and counting the diffracted X-rays caused by the constructive interference of incident rays. The identification can be made by contrasting the d-spacing with accepted reference patterns (Du et al., 2016). Figure 2.4 shows the results

of XRD analysis on CCTO powder at different calcination temperature (Karim et al., 2017).

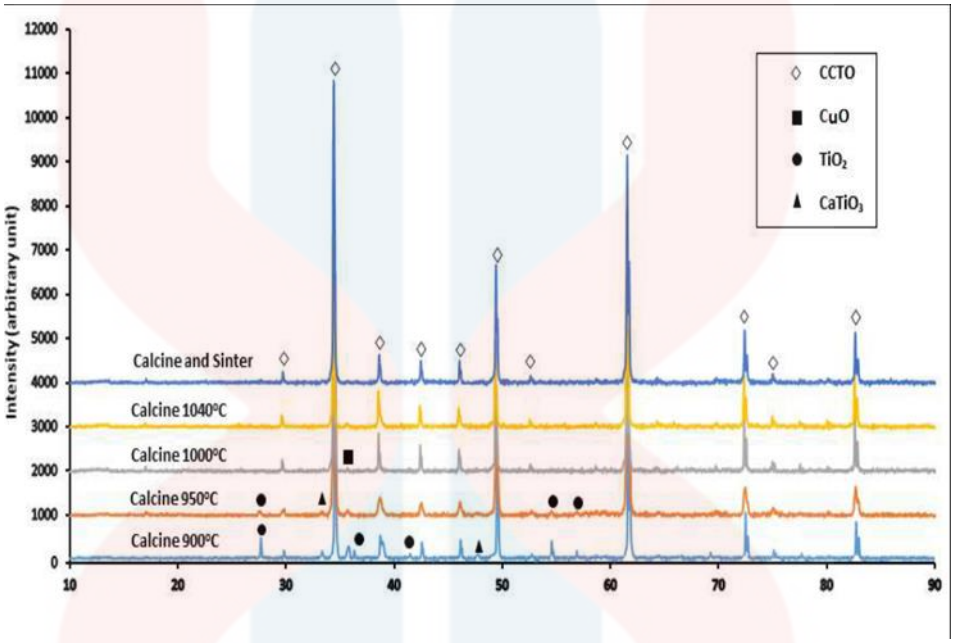

Figure 2.4: XRD pattern for the calcined at different temperature and control calcined-sintered sample.

Source: (Karim et al., 2017)

2.7.2 Dielectric Properties

Dielectric constant, also referred to as relative permittivity and the capacity of a material to carry alternating current in vacuum, is a physical property. According to Figure 2.5, the CCTO's dielectric constant is beginning to decrease as frequency increases. Due to the nature of the polarisation types, CCTO polarisation will lose its effectiveness at higher frequencies. Due to space charging, it is thought that the high dielectric constant of the CCTO originated from the internal boundary layer capacitor (IBLC) (Sulaiman et al., 2010).

.

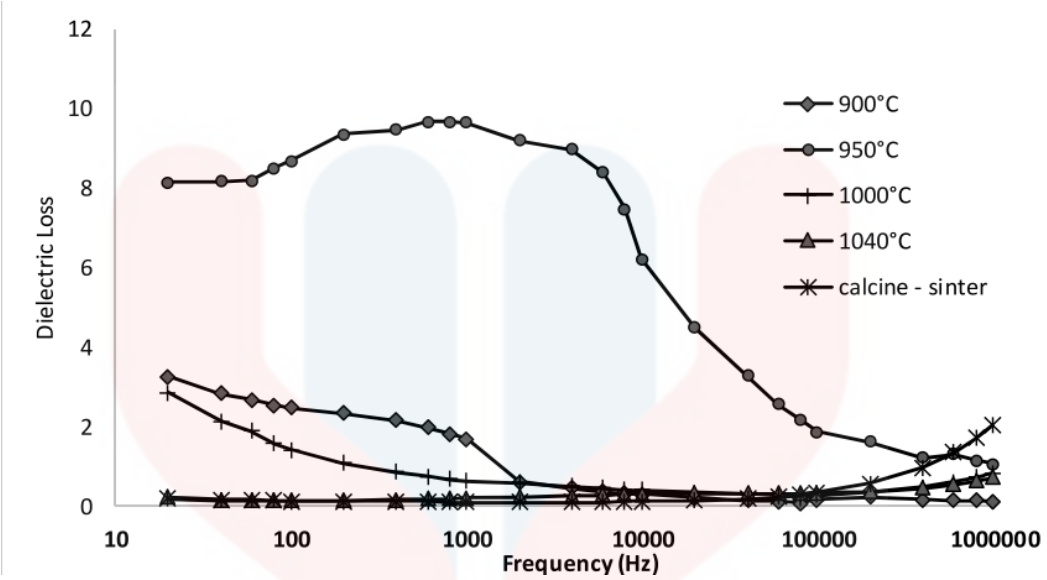

Figure 2.5: Dielectric constant at different calcination temperature

Source: (Karim et al., 2017)

Additionally, for effective energy storage, a dielectric material must also have a low loss tangent in addition to a high dielectric constant. According to Subramanian et al. (2000)'s as shown in Figure 2.5 **Error! Reference source not found.**, the dielectric constant and loss tangent values are roughly constant at temperatures between 80 and 220℃. Additionally, based on Wan et al., (2018) discovered, as stated in his article, that the CCTO/Polyurethane composite's dielectric constant could reach 35.2 at 100 Hz with 40 vol% of CCTO filler.

As a result, the data can be analysed using the Impedance Spectroscopy (IS) instrument, which is the simplest and most practical method for determining the values of the dielectric constant and tangent loss but has a limited range of sensitivity. By varying the voltage across a sample and a standard resistor in a series circuit, impedance determines resistivity. Measurements of the in and out of the voltage were made, and

the amount of current was divided by those measurements to determine the amount of information required. LCR metres are an additional option to the IS instrument for measuring dielectric properties.

2.7.3 Microstructure Analysis

Because small capacitive components allow for the possibility of electronic device size reduction, high dielectric constant materials are widely used in microelectronic devices (Negi et al., 2019). High dielectric constant (r) and low dielectric loss (tan) are characteristics of perovskite ferroelectrics based on barium titanate ($BaTiO_3$, BT). At transition temperature (T_C), which is higher than room temperature (RT), they do have a maximum value of r, and the sharp phase transition at TC has highly temperature-sensitive dielectric properties (Li et al., 2014). Additionally, this system undergoes multiple phase transitions, which makes the dielectric properties temperature dependent, which is undesirable for device applications.

By preparing BT system solid solutions with other compounds that have temperature independent dielectric properties, the temperature stability of the system's dielectric properties can be improved. By adding small concentrations of doping materials, the crystal structure, microstructure, and dielectric properties of BT ceramics can all be enhanced (Negi et al., 2019).

$CaCu_3Ti_4O_{12}$, also known as CCTO, is a non-ferroelectric perovskite material with an enormous value of r at room temperature. This system demonstrates the high value of r, which is independent of frequency (10^2-10^6 Hz) and nearly constant in the temperature range of 100-600 K. The high value of r is 10^4-10^5. Between 35 and 1273 K, CCTO ceramics don't undergo any phase transitions or changes in their crystal

structure (Mu et al., 2009). Extrinsic effects are used to explain why the CCTO system has a high dielectric constant. An internal barrier layer capacitance (IBLC) model is the widely accepted explanation for high r in non-ferroelectric ceramics (Rahman et al., 2016). The grain-boundary IBLC effect in the CCTO system is connected to the giant dielectric response in this model. The IBLC model is applicable to ceramics that exhibit electrical microstructural heterogeneity, where the grain boundaries are significantly more resistive than the grains, leading to high capacitance and, ultimately, a large system permittivity (Haque et al., 2021).

The tan θ of these high-R non-ferroelectric materials is too high, which prevents their use in practical applications despite the apparent importance of their potential uses. The use of materials with high r, low tan θ, and good temperature and frequency stability over a wide range is therefore highly desired (Abdelal et al., 2012).

The behaviour of CCTO and BT must be investigated, which requires the microstructure analysis. Scanning electron microscopy (SEM) will be used for microstructure analysis. The signals generated by the specimen's interaction with the electron beam, which is based on the electron-matter interaction principle, are what determine how an image forms in the SEM. Other types of electrons, such as secondary electrons, X-rays, backscattered electrons, Auger electrons, and others, will be produced by the electron interaction with the specimen. When tungsten filament is subjected to high energy, electrons are produced and released. The schematic diagram of the SEM and the parts that contribute to the imaging picture produced by the electron emission are shown in Figure 2.6.

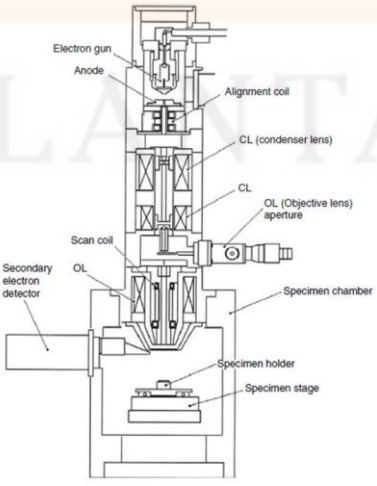

Figure 2.6: Schematic diagram of scanning electron microscope

Source: (Zhou et al., 2007)

X-ray energy dispersive spectroscopy (XEDS) was utilised to investigate the chemicals present in the BT and CCTO composite because SEM only provides image analysis. As seen in Figure 2.7, the typical spectrum of the XEDS profile analysis produced a plot of counts versus X-ray energy. Since each atom produces its own x-ray radiation energy, which is derived from atom orbitals within the atom, the detection was carried out using an EDS detector.

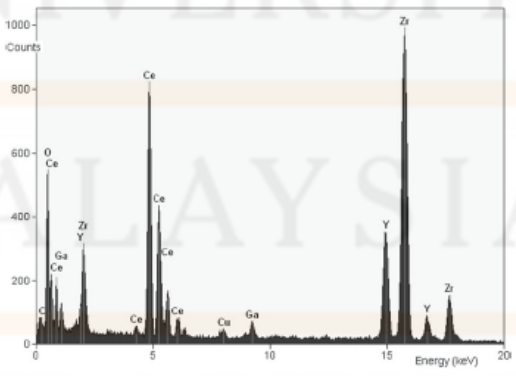

Figure 2.7: An illustration of an XEDS from a sample with up to 20 keV of CeO_2 and YSZ

Source: (Ariga, 2014)

CHAPTER 3

MATERIALS AND METHODS

3.1 Introduction

The study encounters the ceramic matrix composite, and the work was done in two stages as shown in the flowchart in Figure 3.1. Stage 1 for synthesising Calcium Copper Titanate ($CaCu_3Ti_4O_{12}$, CCTO) and Barium Titanate ($BaTiO_3$) powder through solid states reaction method. Stage 2 for mixing CCTO powder with $BaTiO_3$ and characterisation of the compound. The starting materials used to synthesise CCTO and $BaTiO_3$ is $CaCO_3$, CuO, $BaCO_3$ and TiO_2, methanol as grinding medium and zirconia ball as milling media. Then, $BaTiO_3$ with CCTO and another additive were mixed in an internal mixer and analyse the sample. The total samples prepared are 6 samples, which differs in BT/CCTO content with parameter. Therefore, the samples were characterised by X-ray diffraction for CCTO and BT powder. Meanwhile, for CCTO/BT composite the characterisations were done by X-ray diffraction, scanning electron microscope/energy dispersive spectroscopy, density and porosity measurement and thermogravimetric analysis.

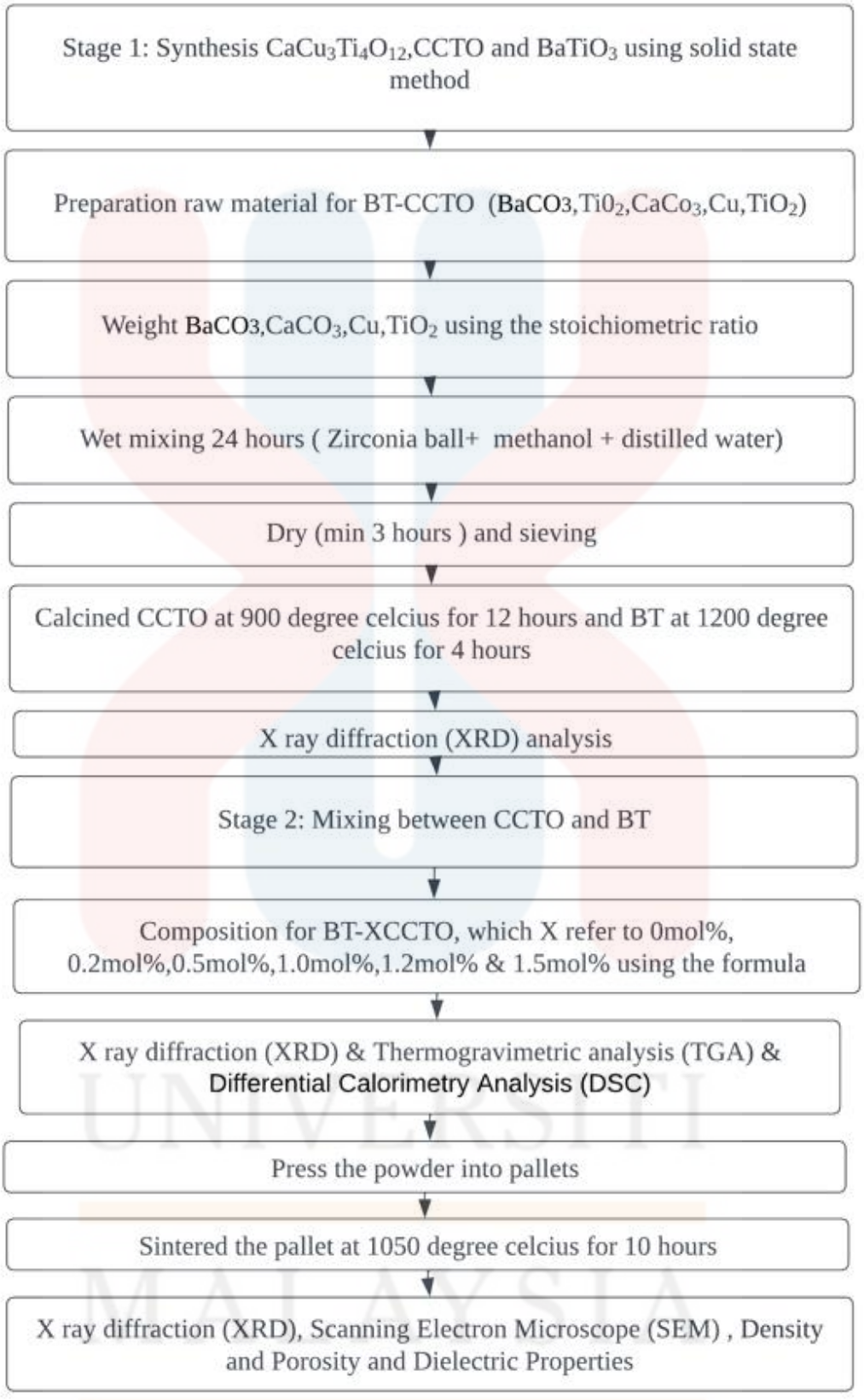

Figure 3.1: Flowchart of CCTO/BT processing and analysis.

Stage 1 for CCTO and BT preparation and Stage 2 for composition of CCTO with BT.

3.2 Raw Material for $CaCu_3Ti_4O_{12}$ Powder Preparation

The starting materials, stoichiometric ratio calculation, and temperature processing used in this study's solid-state reaction of CCTO powder are all described in detail.

3.2.1 Copper (II) Oxide

Copper (II) oxide (CuO) is the second major contributor in synthesising CCTO powder after TiO_2. CuO was supplied by R&M Chemicals (CAS:1317-38-0, 500g) >95.0% purity and for laboratory and industrial use only. The molecular weight of CuO is 79.55 g/mol, and the power appears in black coloured powder.

3.2.2 Titanium Dioxide

The most abundance or major raw material in synthesise CCTO powder is titanium (IV) oxide or its commercial name titanium dioxide (TiO_2). TiO_2 was supplied by R&M Chemicals (CAS:13463-67-7, 500g) with 99.5% purity and analytical reagent (A.R.) grade. The molecular weight of TiO_2 is 79.87 g/mol, and the power appears in white coloured powder.

3.2.3 Calcium Carbonate

Calcium carbonate ($CaCO_3$) was used as raw material to synthesis CCTO, instead of using calcium oxide (CaO) due to the unstable element and very reactive toward the environment. $CaCO_3$ was supplied by R&M Chemicals (CAS:471-34-1,

1000g) with 99.0% purity and analytical reagent (A.R.) grade. The molecular weight for $CaCO_3$ is 100.09 g/mol. The physical appearance of powder is white coloured powder.

3.2 Raw Materials for $BaTiO_3$ Powder Preparation

The starting materials, stoichiometric ratio calculation, and temperature processing used in this study's solid-state reaction of $BaTiO_3$ powder are all described in detail.

3.3.1 Barium Carbonate

Barium carbonate ($BaCO_3$) was used as raw material to synthesis $BaTiO_3$, instead of using barium oxide (BaO) due to the unstable element and very reactive toward the environment. $BaCO_3$ was supplied by R&M Chemicals (CAS:513-7-9,500g) with purity 98.5% purity and analytical reagent (A.R.) grade. The molecular weight for $BaCO_3$ is 84.63g/mol. The physical appearance of powder is white coloured powder.

3.3.2 Titanium Dioxide

The most abundance or major raw material in synthesise $BaTiO_3$ powder is titanium (IV) oxide or its commercial name titanium dioxide (TiO_2). TiO_2 was supplied by R&M Chemicals (CAS:13463-67-7,500g) with 99.5% purity and analytical reagent (A.R.) grade. The molecular weight of TiO_2 is 34.25 g/mol, and the power appears in white coloured powder.

3.4 Synthesise of Calcium Copper Titanate ($CaCu_3Ti_4O_{12}$) Powder Through Solid-State Reaction

Based on the chemical reaction of CCTO as shown in Equation 3.1, the calculation of stoichiometric for the raw materials used was done in Table 3.1 for production of every batch (100 g of CCTO). The total weight of raw materials needed was 100 g, with 7.16 g by-product was released as CO_2 gas during calcination process.

$$CaCO_3 + 3CuO + 4TiO_2 \rightarrow CaCu_3Ti_4O_{12} + CO_2 \quad \text{Equation 3.1}$$

Table 3.1: Amount of raw material used for 100g preparation of CCTO, and number of by-products produced.

Sample used	Molecule Weight (g/mol)	Mass (g)
$CaCO_3$	100.086	16.30
CuO	79.545	38.85
TiO_2	79.866	52.01
Final product produce:		
$CaCu_3Ti_4O_{12}$	614.179	100.00
CO_2	44.010	7.16

3.4.1 Weighing

The first step is to weigh the raw material. Therefore, the amount of CuO, $CaCO_3$ and TiO_2 as referring to the Table 3.1, 1000g of Zirconia ball was weighted using mechanical balance in Material Science laboratory. Then, 50 ml of methanol and distilled water were measured using a measuring cylinder. The calculation of CCTO can refer to Appendix A.

3.4.2 Milling and Mixing

Milling and mixing is an important process to decrease particle size and preventing aggregation. Additionally, it seeks to create a highly homogeneous raw material mixture. The matter of next to particles must interdiffusion for compound formation to occur during calcination or firing, and the amount of time needed to finish the process will be equal to the square of the particle size (Mu et al., 2009). In comparison to larger sizes, the smaller particles have a larger surface area. As a result, the smaller size has a faster diffusion rate than the larger size. Magna 33 Value Sdn Bhd provided a Lab Roll Mill (type no. QM-5) that was used to mix the compound in PU jars for 24 hours at 120 rpm which allow enough time for homogeneity to take place.

3.4.3 Methanol

Wet milling is more favourable compared to dry milling because wet milling will speed up the homogenising process. Therefore, methanol (CH_3OH) is used as grinding medium to assist the $CaCO_3$, CuO and TiO_2 powder for rapidly homogenous. It was supplied by Avantor (J.T.Baker® brand) (CAS: 67-56-1-4000ml) with purity >99.8%. A disadvantage of wet milling is time-consuming for the drying process.

Besides, the handling of methanol should be done in a fume hood since it can easily evaporate and could lead harm to human being.

3.4.4 Distilled Water

Distilled water is used as a solvent to dilute methanol concentration. This distilled water is free from contaminant and produced by Faculty Bioengineering and Technology's laboratory.

3.4.5 Polyyurethane Mill Jar

The PU (polyurethane) mill jar a polymer-type jar with a volume of 1500 ml, an outer diameter of 132 mm, an inner diameter of 116 mm, and a height of 161 mm was used in this investigation. A high-quality product from an effective milling process requires that the jar content utilise up to two thirds of the jar volume. The raw material and grinding media will stick together because there won't be enough room for them to move if the content filled has more than that.

3.4.6 Zirconia Ball

The milling media for this study is zirconia (ZrO2) balls with varies diameter as shown in Figure 3.2 that was supplied by Magna Value Sdn Bhd. The proportion or ratio of raw materials with the ball is 1:10. So, the total weight of zirconia balls used in this study ±1000 g since. In addition, zirconia balls are chemically stable (produce high purity of sample) even at high temperature. Zirconia balls are also high hardness and wear resistant than alumina balls. Zirconia balls can be easily recognised due to the shiny appearance compared to alumina balls.

Figure 3.2: Zirconia ball used

3.4.7 Drying and Sieving

The grey-coloured wet mixture was milled and mixed, then allowed to dry in a fume hood for three to five hours in a beaker. The compound was sieved using a standard sieve once it had completely dried. To create finer powders, the large particle was lastly ground up using an agate mortar.

3.4.8 Calcination

The calcination process typically occurs at a temperature lower than that of sintering. The powders were calcined at 900°C for 12 hours in an alumina crucible, as shown in Figure 3.3 using furnace. After calcined, the CCTO powder then crushed with agate mortar to prevent from the powder from agglomerate.

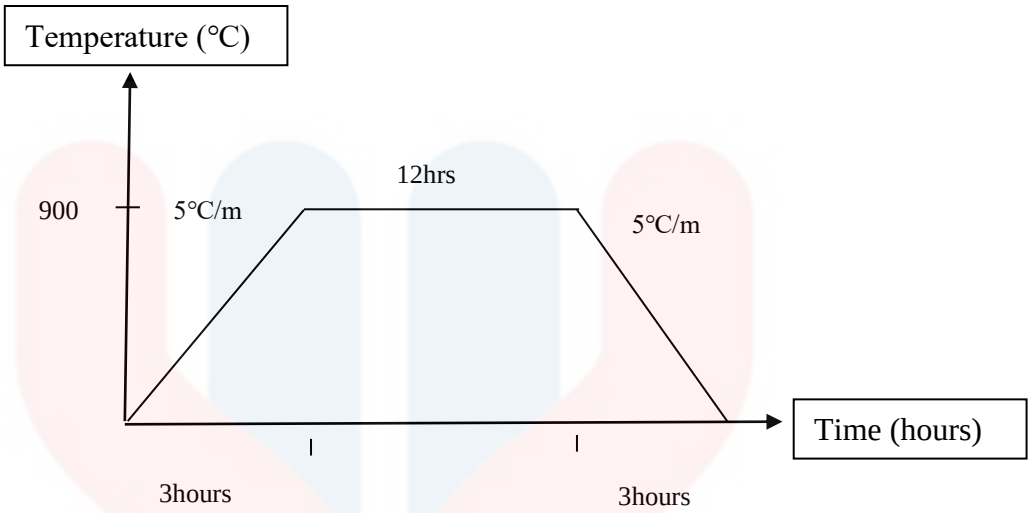

Figure 3.3: Heating profile for CCTO calcination process.

3.5 Synthesise of Barium Titanate (BaTiO3) Powder Through Solid State Reaction

Based on the chemical reaction of $BaTiO_3$ as shown in Equation 3.2, the calculation of stoichiometric for the raw materials used was done in Table 3.2 for production of every batch (100 g of $BaTiO_3$). The total weight of raw materials needed was 100 g, with 10.748 g by-product was released as CO_2 gas during calcination process. Meanwhile, for BT, the calculation of stoichiometric for the raw material used was done in Table 3.2.

$$BaCO_3 + TiO_2 \longrightarrow BaTiO_3 + CO_2 \qquad \text{Equation 3.2}$$

Table 3.2: Amount of raw material used for 100g preparation of BT, and number of by-products produced.

Sample used	Molecule Weight (g/mol)	Mass (g)
$BaCO_3$	197.338	84.63
TiO_2	79.866	34..25
Final product produce:		
$BaTiO_3$	233.176	100.00
CO_2	44.01	7.16

3.5.1 Weighing

The first step is to weigh the raw material. Therefore, the amount of CuO, $CaCO_3$ and TiO_2 as referring to the Table 3.1, 1000g of Zirconia ball was weighted using mechanical balance in Material Science laboratory. Then, 50 ml of methanol and distilled water were measured using a measuring cylinder. The calculation of CCTO can refer to Appendix A.

3.5.2 Milling and Mixing

Reducing particle size and avoiding aggregation were largely dependent on the milling and mixing process. It also aims to produce a very homogenous mixture of raw materials. The smaller particles have more surface area than the larger ones. The smaller size thus has a faster rate of diffusion than the larger size. The compound was mixed in

PU jars for 24 hours at 120 rpm using a Lab Roll Mill (type no. QM-5) supplied by Magna 33 Value Sdn Bhd, which allowed enough time for homogeneity to occur.

3.5.3 Drying and Sieving

After milling and mixing the white-coloured wet mixture, it was left in a beaker to dry for three to five hours under a fume hood. When the compound was completely dry, it was sieved through a regular sieve. The large particle was lastly ground up with an agate mortar to produce finer powders.

3.5.4 Calcination

Usually, the calcination process takes place at a lower temperature than the sintering process. The powders were calcined in an alumina crucible using a furnace set at 1200°C for 4 hours, as shown in Figure 3.4. To stop the BT powder from accumulation together, it was first calcined and then crushed using an agate mortar.

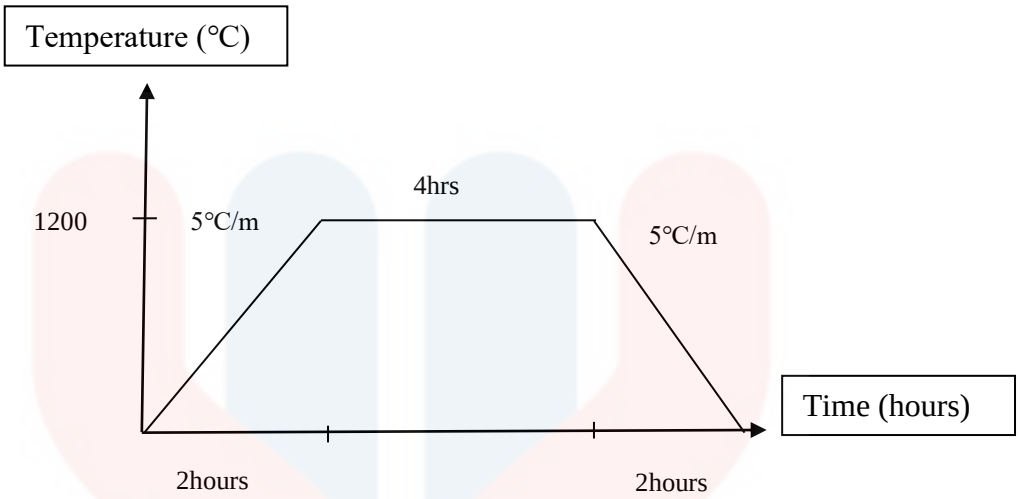

Figure 3.4: Heating profile for BT calcination process

3.6 Characterization of Calcium Copper Titanate ($CaCu_3Ti_4O_{12}$) and Barium Titanate ($BaTiO_3$) Powder

3.6.1 X-ray diffraction (XRD) Analysis

A non-destructive method of analysing crystal structures and identifying phases in crystal structures is called X-ray diffraction (XRD), and it works by applying Bragg's Law. The analysis was conducted using the Bruker D2-Phaser XRD machine, which is in the UMK X-ray laboratory. To begin with, powders were ground into fine powder. Then, to avoid preventing the crystal's preferred orientation, the powder of the CCTO and BT was placed on the sample holder and gently flattened within the sample holder cavity without compressing them. Subsequently, the sample was subjected to CuKα radiation and scanned for 2θ between 10 and 90. Next, DIFFRAC.EVA software was used to analyse the powder diffraction pattern results.

3.7 Calcium Copper Titanate ($CaCu_3Ti_4O_{12}$) and Barium Titanate ($BaTiO_3$) Composite Preparation

3.7.1 Weighing

BT and CCTO powder were weighted based on the stoichiometry ratio in Equation 3.3 where the x = 0, 0.2, 0.5, 1.0, 1.2, and 1.5 mol%. The weight of each composition is shown in Table 3.3. The calculation for each composition was attached in Appendix B.

$BaTiO_3.xCaCu_3Ti_4O_{12}$ Equation 3.3

Table 3.3: Composition of $BaTiO_3.xCaCu_3Ti_4O_{12}$

Composition (X mol%)	**0**	**0.2**	**0.5**	**1.0**	**1.2**	**1.5**
Calculated weight of BT (g)	20	13.1	8.6	5.5	4.8	4.0
Calculated weight of CCTO (g)	0	6.9	11.4	14.5	15.2	16.0

3.7.2 Milling and mixing

In a ball mill, each composition as CCTO and BT was mixed for 16 hours at 120 rpm. To a polyethylene container containing zirconia balls as the grinding media, stoichiometric amounts of the precursors were added at a 1:10 powder to ball ratio.

3.7.3 Drying and sieving

The brown coloured mixture was mixed and ground, and then it was placed in a beaker under a fume hood to dry for three to five hours. The compound was sieved using a standard sieve after it had dried completely. To create finer powders, the large particle was lastly ground up using an agate mortar.

3.7.4 Calcination

The temperature at which the calcination process occurs is typically lower than that of the sintering process. As illustrated in Figure 3.4, the powders were calcined in an alumina crucible for four hours at 1200°C in a furnace. Using an agate mortar, the BT and CCTO powder was first calcined and then crushed to prevent it from clumping together.

3.7.5 Pressing process

The result was ground into a fine powder using an agate mortar. WD-40 was used to clean the mould wall and get rid of any contamination and rust. The CCTO and BT calcined powder was then combined, and the mixture was compressed into pellets with a diameter of 2 mm and a size of 10 mm using uniaxial compression and 300 MPa pressure for two minutes.

3.7.6 Thermogravimetric Analysis (TGA) and Differential Calorimetry Analysis (DSC)

Both TGA and DSC analyses can be completed simultaneously. Figure 3.5 illustrates the TGA/DSC 2 model of Mettler Toledo's equipment, which was used to test the CCTO/BT samples. The samples were weighed using a crucible to approximate a weight of 0.026–0.028 g before testing. Once inside the testing chamber, the samples were heated at a rate of 10°C per minute and the gas flow was set to 50 millilitres per minute. Utilising air gas, the samples were examined between room temperature (27°C) and 900°C. STAR^{e} evaluation software was utilised for the data and results analysis.

Figure 3.5: TGA/DSC instrument (Mettler Toledo, model; TGA/DSC 2)

3.8 Composite Characterization Calcium Copper Titanate ($CaCu_3Ti_4O_{12}$) and Barium Titanate ($BaTiO_3$)

The composite of CCTO with BT at different mol% were characterised using XRD, density, and SEM. The method of testing is described in the following section.

3.8.1 X-ray diffraction (XRD) analysis

X-ray diffraction (XRD) is a useful non-destructive method for characterising crystalline materials. Structures, phases, preferred crystal orientations (texture), and other structural characteristics like average grain size, crystallinity, strain, and crystal defects are all covered. The phase formation of the CCTO and BT composite was determined by the XRD test. The phase of each peak was then labelled.

3.8.2 Density and Porosity Test

A density testing machine was used to measure the density. The testing machine used buoyancy technique which is known as Archimedes Principle. Both air and liquid media were used to weigh the sample. This demonstrates the Archimedes Principle, according to which an object submerged in liquid experiences a decrease in apparent weight equal to the weight of the liquid's displacement volume. Water was utilised as the liquid medium in this investigation because 1ml of it has a mass of precisely 1g. Then, the relative density of each sample was calculated by using Equation 3.4.

$$\dot{\rho}s = \dot{\rho}_{fl}\frac{m\,(a)}{m(a)-m(fl)} \qquad \text{Equation 3.4}$$

Where,

$\dot{\rho}s$ = Density of body

$\dot{\rho}_{fl}$ = Density of Liquid

$m_{(a)}$ = Mass of Body

$m_{(fl)}$ = Mass of Liquid

The porosity calculated by using Equation 3.5

$$\pi_a = \frac{m3-m1}{m3-m2} \times 100 \qquad \text{Equation 3.5}$$

π_a = porosity

m_1= mass of the dried sample

m_2=apparent mass of saturated sample in water

m_3=Mass of saturated sample weight in air

3.8.3 Scanning Electron Microscopic (SEM) and Energy-dispersive X-ray spectroscopy (EDX)

Using a scanning electron microscope (SEM) (JEOL; model JSM-IT100) in the Faculty of Earth Science laboratory, the morphology properties of CCTO/BT were examined. It takes careful sample preparation to obtain high-quality imaging. Both the sample and the holder were covered with carbon double tape. To prevent static charge from building up at the sample surface, the conductive carbon tape served as an excessive charge conductor to the ground.

Figure 3.6: Scanning Electron Microscopic (SEM) and Energy-dispersive X-ray Spetroscopy (EDX) (JEOL; model JSM-IT100)

3.8.4 Inductance, Capacitance and Resistance (LCR) meter

LCR meter is a tool or apparatus for measuring the CCTO/BT composite's capacitance (Farad) and dissipation factors in relation to frequency. Before that, each composite was grinded and polished using sandpaper. After polished, the sample were smudged with silver phase.The samples analysis was conducted using precision LCR meter (Novocontrol Technologies; model D-56414) as shown in Figure 3.7, which is in Institute Nano electric and Electronic (INEE), University Malaysia Perlis (UniMAP), Perlis

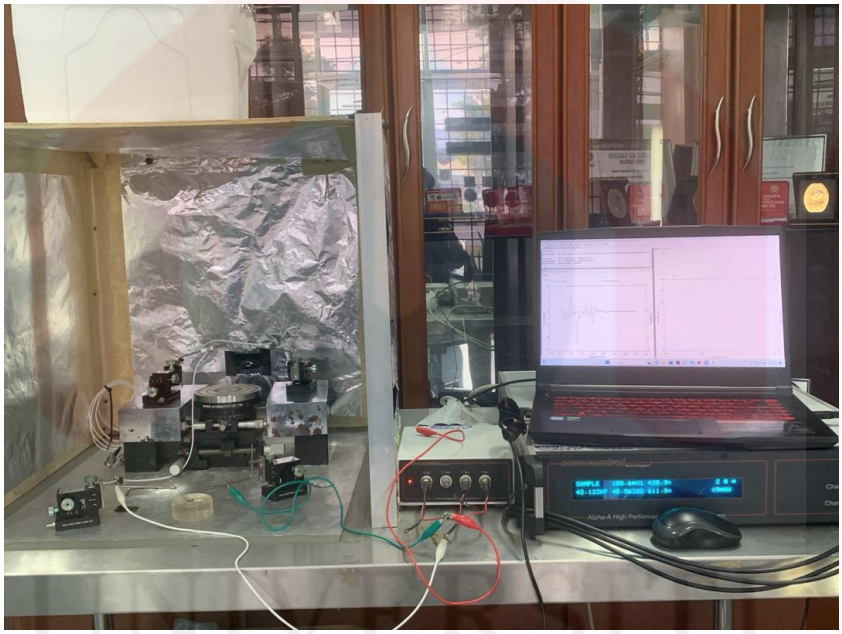

Figure 3.7: LCR meter (Novocontrol Technologies; model D-56414

By placing a sample between two electrodes and applying sinusoidal voltage (alternating current) to the electrodes at a frequency range of 100 kHz to 10 MHz, the samples were tested at room temperature.

The dielectric constant of the materials was calculated using Equation 3.5, then graphs of dielectric constant, ε_r versus frequencies were plotted. While the graphs for dissipation factor value were directly constructed from the data.

$$\varepsilon_r = \frac{tC}{\varepsilon_\circ A} \qquad \text{Equation 3.5}$$

Where,

A: Cross area

t: Thickness

C: Capacitance

$\varepsilon_\circ$: Universal Constant (8.85×1012 F/m)

ε_r: Dielectric constant

CHAPTER 4

RESULTS AND DISCUSSION

4.1 Introduction

In this chapter, several testings were conducted for characterisations and analyses of the sample to ensure the purity and quality itself. The characterisations were carried out based on the flowchart in Figure 3.1. The first stage started with the characterisation of CCTO and BT using X-ray Diffraction (XRD) and Thermogravimetric Analysis (TGA) and Differential Calorimetry Analysis (DSC) to make sure a complete reaction occurs during synthesis and to control the particle size. The second stage is to determine the effect of composition BT and CCTO on mechanical, morphology, and dielectric properties of the composite produced.

4.2 Synthesised of Calcium Copper Titanate ($CaCu_3Ti_4O_{12}$) and Barium Titanate ($BaTiO_3$) Powder

4.2.1 X-ray Diffraction (XRD)

In this section, the properties of CCTO and BT powder were characterized regarding their phase formation by XRD.

4.2.1.1.1 $CaCu_3Ti_4O_{12}$ Powder

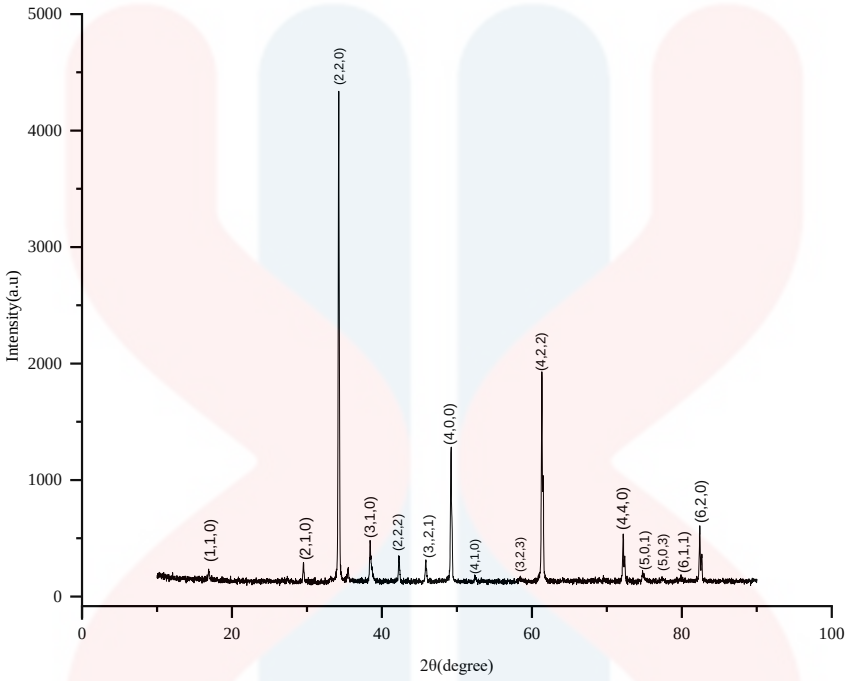

Figure 4.1: XRD Pattern for CCTO Powder

As shown in Figure 4.1, the observed peak of CCTO matched COD 1532158 attached in Appendix C(a); there were no secondary peaks or residual starting materials. Through a calcination process, CCTO powder was successfully synthesised from a mixture of initial raw materials using the solid-state reaction method. The mixture's colour changed from grey to brown because of this process. To confirm that the reaction during calcination was complete, an XRD analysis was carried out. The Bruker Diffract. EVA software made the process of interpreting the data easier.

According to (Schmidt et al., 2013), the CCTO unit cell, which is commonly indexed as cubic Im^3, is a duplicate simple perovskite cell. The XRD results displayed in Figure 4.1 allow for the identification of the sample's cubic structure. The crystanality for CCTO is 93.9wt%.

4.2.1.1.2 $BaTiO_3$ Powder

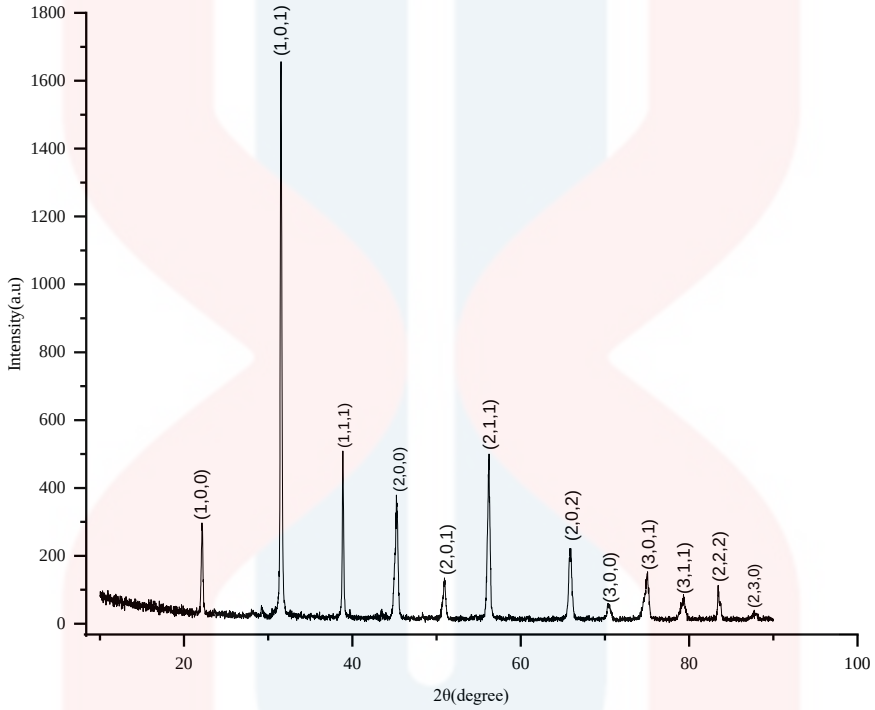

Figure 4.2: XRD Pattern for BT Powder

Figure 4.2 shown the XRD pattern of the BT powder, which was created after four hours of heat treatment at 1200°C. This study's XRD results positively verified that the single BT phase still has a cubic crystal structure. The crystanality for BT is 92.7wt%. The powder became white after the calcination process. As seen in Figure 4.2, the measured peak of the single phase of BT matched COD 1507757 attached in Appendix C(b).

4.3 Composite Preparation Calcium Copper Titanate ($CaCu_3Ti_4O_{12}$) and Barium Titanate ($BaTiO_3$)

In this section, the properties of mix between BT/CCTO were discussed.

4.3.1 X-ray Diffraction (XRD)

XRD analysis was performed on the mixture powders with varying CCTO compositions, as shown in Figure 4.3. In the XRD, the elevated CCTO mol% led to a rise in CCTO peaks and, conversely, a decrease in the BT peak. To determine the homogeneity following milling and to measure this composition amount, semi-quantitative (S-Q) XRD analyses were performed.

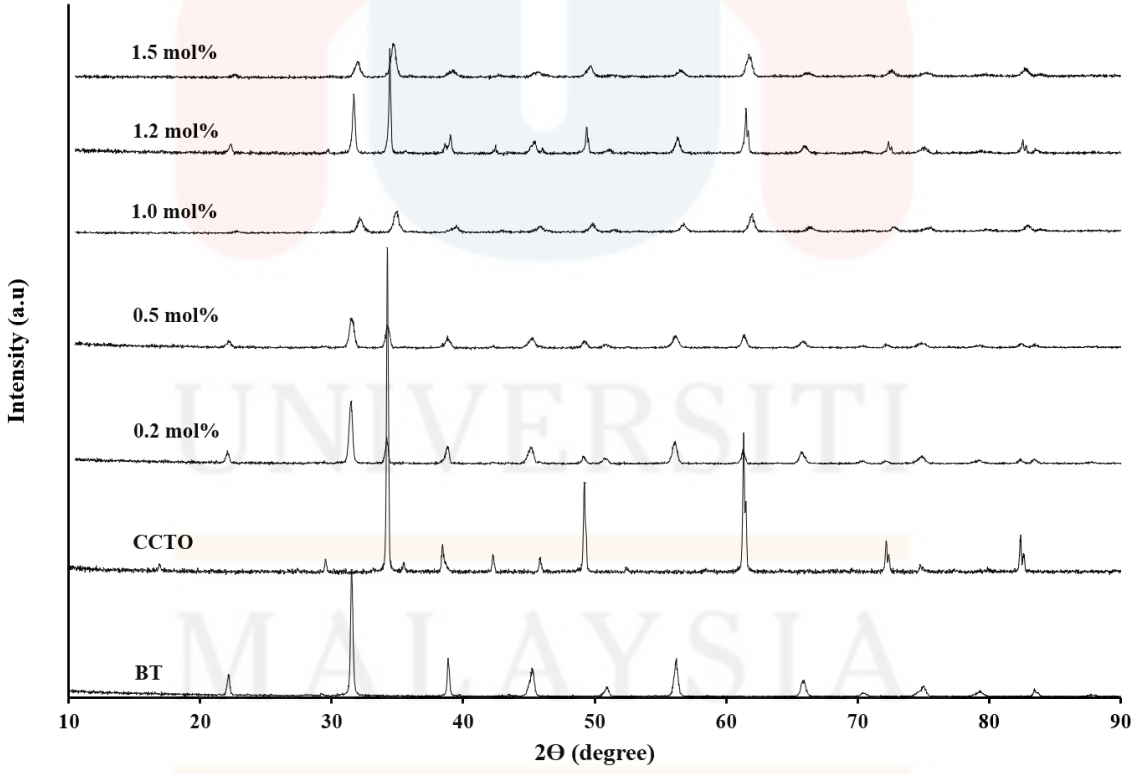

Figure 4.3: Composition of BT/CCTO mixture

Figure 4.4 demonstrates the weight percentage comparison result from the weighted samples prior to the ball mill and the S-Q analysis following the milling. This is simply a small distinction between the two circumstances. To close the gap and make sure the samples have the expected compositions, it is suggested that the sample be larger (20g or more) or that the milling time be extended (16 hours or more). Among the samples, the BT consistently noted a lower weight percentage from the S-Q result than the weight percentage prior to milling. Since BT compound diffuses more slowly during milling than CCTO does, it is impossible for CCTO to have a weight percentage after milling that is higher than the weight percentage before milling. This is expected to result in variation or inhomogeneous sampling for S-Q results.

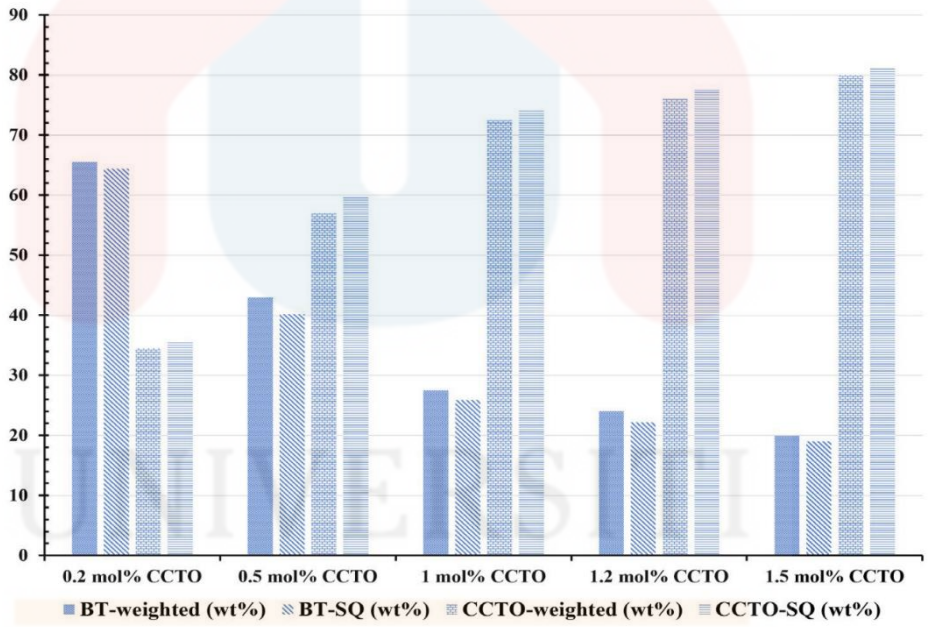

Figure 4.4: Comparison of wt% from weighted samples and S-Q analysis

4.3.2 Thermogravimetric Analysis (TGA) and Differential Calorimetric Analysis (DSC)

The results of measurements using differential calorimetric analysis (DSC) and thermogravimetric analysis (TGA) are shown in Figure 4.5. All samples exhibit a drop in weight up to 100°C because of the air's moisture loss. On the other hand, the oxidation process of both compounds may be the cause of the sample weight increase over the temperature range of room temperature to 900°C. Reoxidation during the TGA measurement can result from the creation of a significant quantity of oxygen vacancy during the milling process, as oxidation already happened during the calcination process.

This was further demonstrated by the DSC results from the temperature change, and the heat flow showed that the mixtures of compounds caused the exothermic reaction of oxidation to occur after the early endothermic reaction at about 100°C, which was caused by the evaporation of water inside the sample.

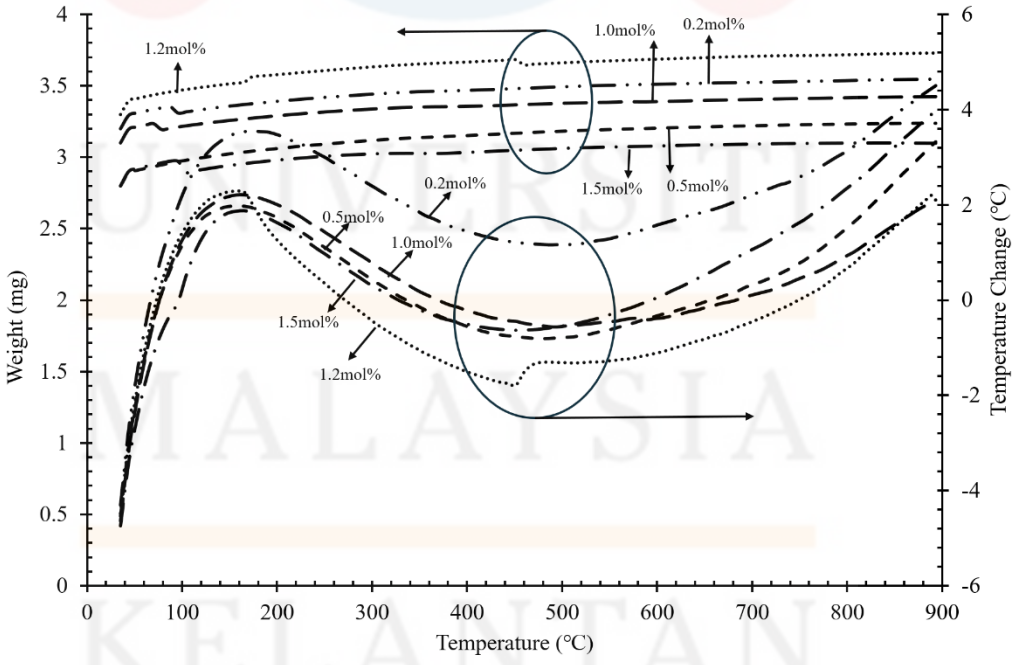

Figure 4.5: Thermogravimetric and differential thermal analysis

4.4 Composite Characterization Calcium Copper Titanate ($CaCu_3Ti_4O_{12}$) and Barium Titanate ($BaTiO_3$)

4.4.1 X-ray Diffraction (XRD)

Figure 4.6 shows the XRD pattern of sintered pellet of CCTO, BT, 0.2mol%, 0.5mol%,1.0mol%,1.2mol% and 1.5mol%. From the graph, the highest intensity is 2709 count. Each peak shows the cubic structure.

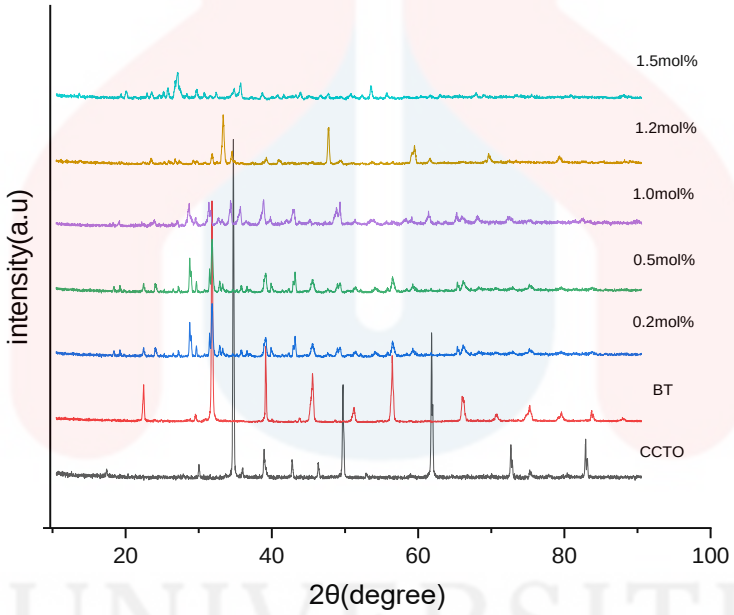

Figure 4.6: XRD Pattern after sintered pallets.

4.4.2 Density and Porosity

Table 4.1 shown the table density and porosity of samples. According to the (Tsuji et al., 2020), the theoretical bulk density for BT is 6.03 g cm^{-3} while according to the (Schmidt et al., 2013) for CCTO is 5.04 g cm^{-3} but in this study BT is 2.15 g cm^{-3} and CCTO is 4.34 g cm^{-3} which are quiet far from the theoretical bulk density. Meanwhile for the composition BT-CCTO the highest is 4.21 g cm^{-3} .This is due to the influence of sintering time and pressure that made it during worked (Petrášek et al., 2021).

Table 4.1: Table density and porosity of samples

Sample (mol%)	In Air	In Water	Bulk Density (g cm^{-3})	Relative Density (%)	Porosity (%)
BT	0.65	0.51	2.15	55.82	61.9
CCTO	0.65	0.51	4.34	86.11	9.45
0.2	0.60	0.46	4.21	47.35	14.5
0.5	0.73	0.55	4.10	46.11	8.08
1.0	0.64	0.47	3.55	39.93	15.3
1.2	0.69	0.52	2.66	29.92	12.79
1.5	0.70	0.53	3.73	41.95	15.73

From the Figure 4.4 shown the trend of density. The highest density among all the composition BT-CCTO is 0.2mol% pallet at 4.21g/cm^3 and the lowest is 1.2mol% pallet at 2.66 g/cm^3. This happened due to where the material was moved from within the grains into the pore microstructure, causing a reduction in the volume of the pores (Majhi et al., 2007).

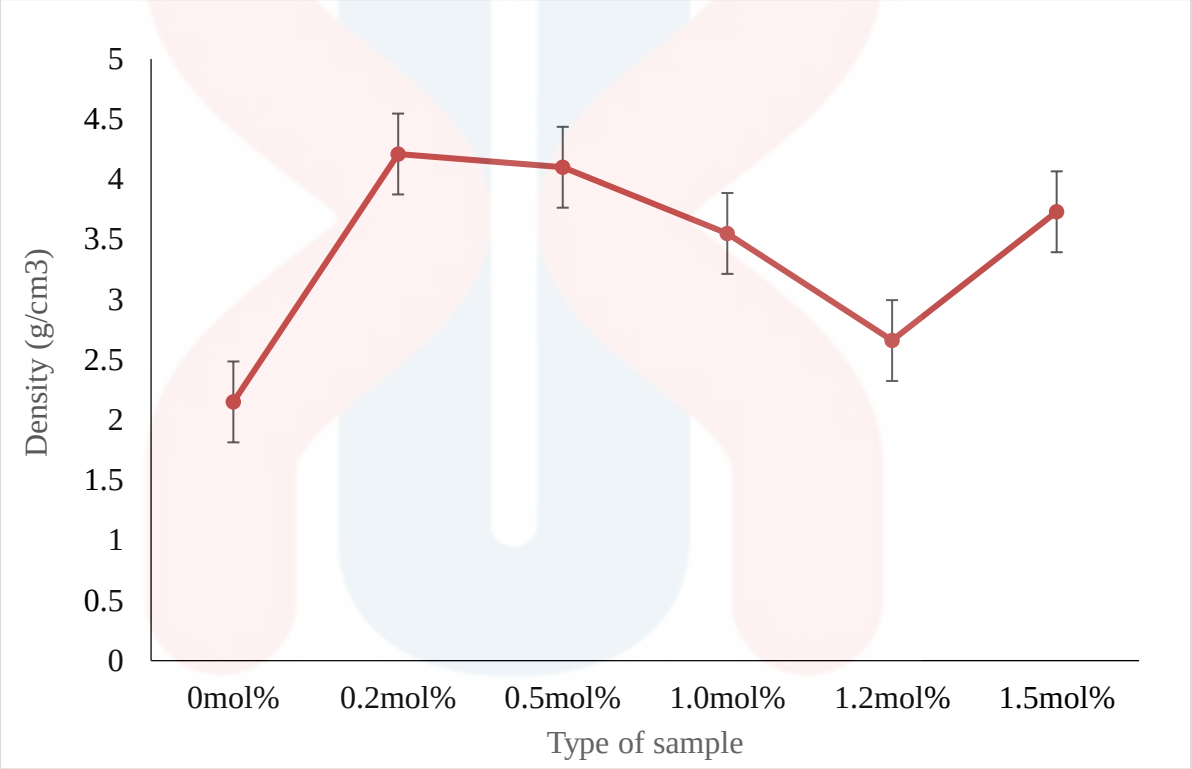

Figure 4.7: Density of Composition CCTO/BT

Figure 4.8 show the porosity that formed in the samples when sintered. Sample 0.5mol% shown the lowest of porosity other than sample. From the graph, can be conclude that the higher density samples proposed the lower porosity.

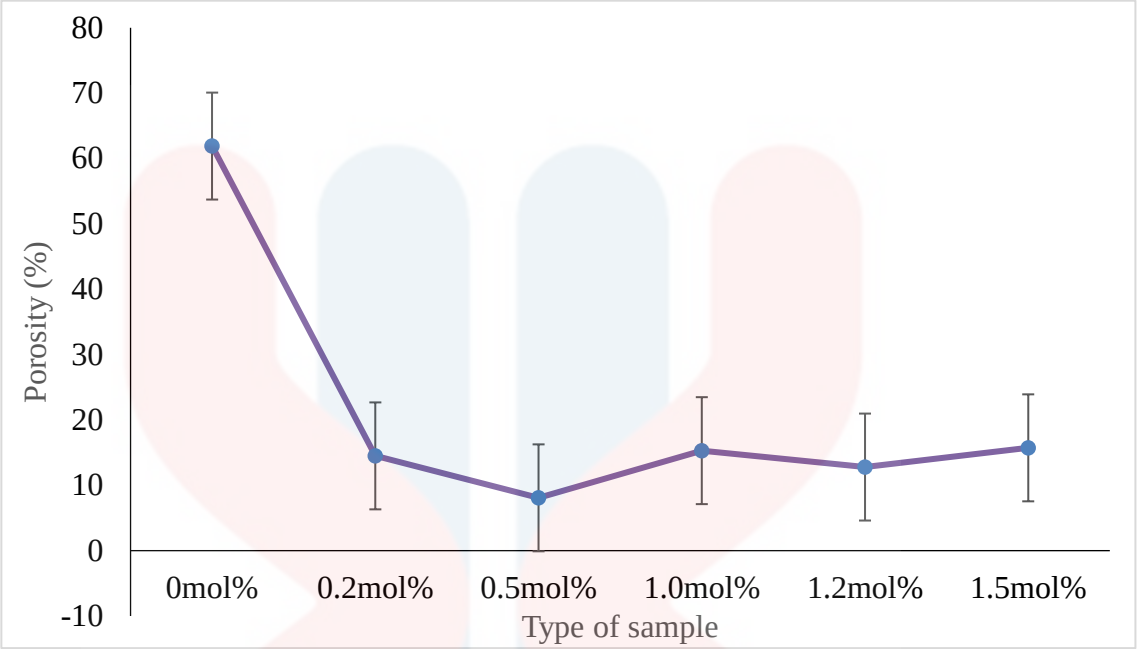

Figure 4.8: Porosity of Composition CCTO/BT

4.4.3 Morphology Properties

Using a scanning electron microscope (SEM), the surface morphology of the cross section of the CCTO/BT composite was examined. Sample preparation is the most important step before analysis because it can impact the imaging quality. Due to the charging effect, unfit sample preparation will lead to poor imaging quality.

Figure 4.9 shows SEM micrographs of the CCTO/BT pellets sintered at 1050℃ for 10 hours with different composition using solid-state method. As observed, the microstructure of CCTO/BT change significantly with the increasing of composition content. It was found that the grain boundaries of CCTO/BT almost covered by the light-coloured exfoliated sheets. When the content from 0.2mol% up to 1.5mol%, the whole grain CCTO/BT were covered. Figure 4.9 (D), it shown that the particle size for CCTO/BT that combined.

To confirm the particle composition, the EDS analysis was used. Figure 4.10 and Figure 4.11 shows the EDS analysis of CCTO/BT with different composition between 0.2mol% until 1.5mol%. EDS analysis shows the raw material elements (Ca, Cu, Ti, O, C and Ba) with composition close to stoichiometric ratio.

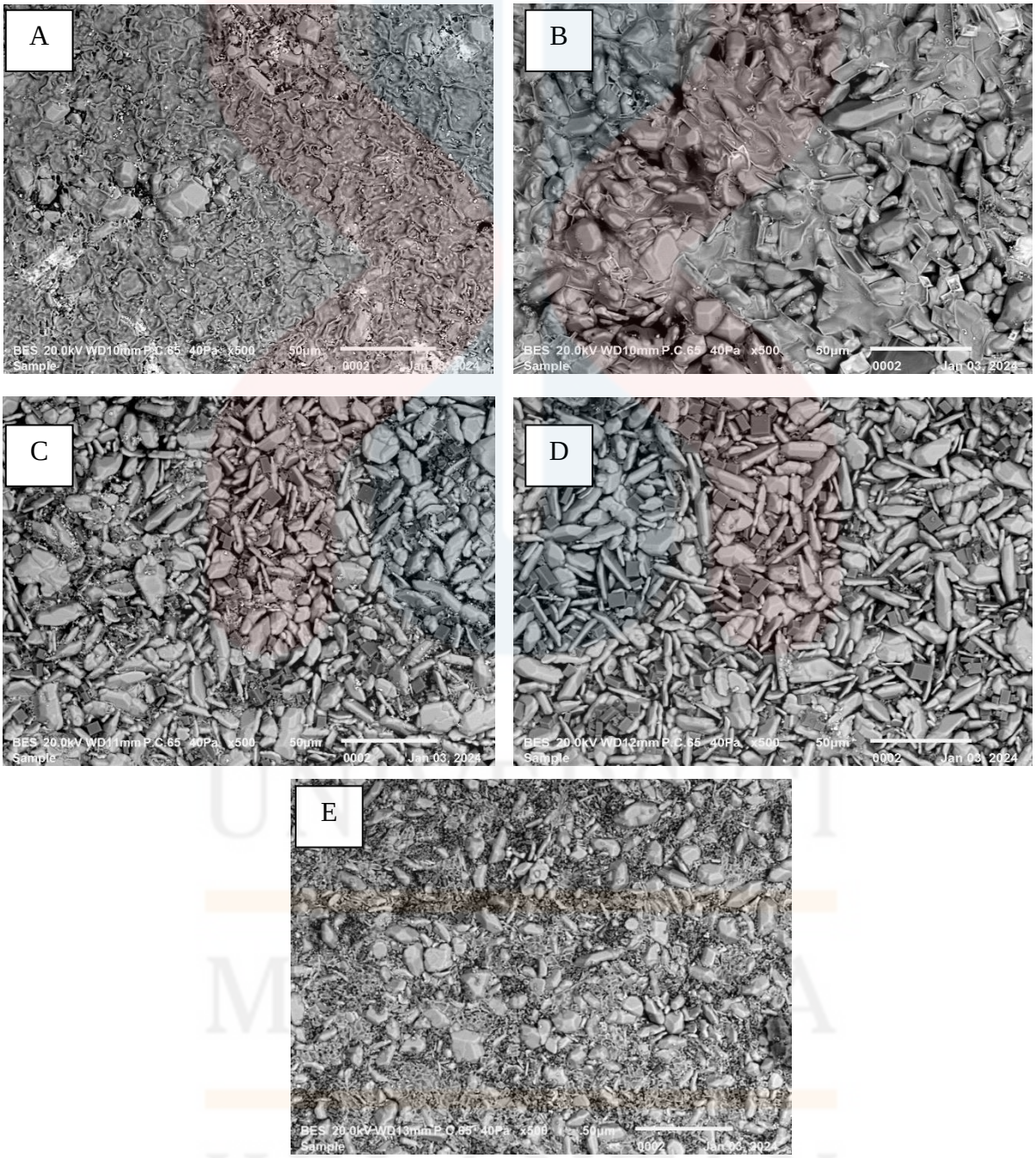

Figure 4.9: Surface morphology on CCTO/BT A) 0.2mol% B)0.5mol% C)1.0mol% D)1.2mol% and E) 1.5mol% using scanning electron microscopy.

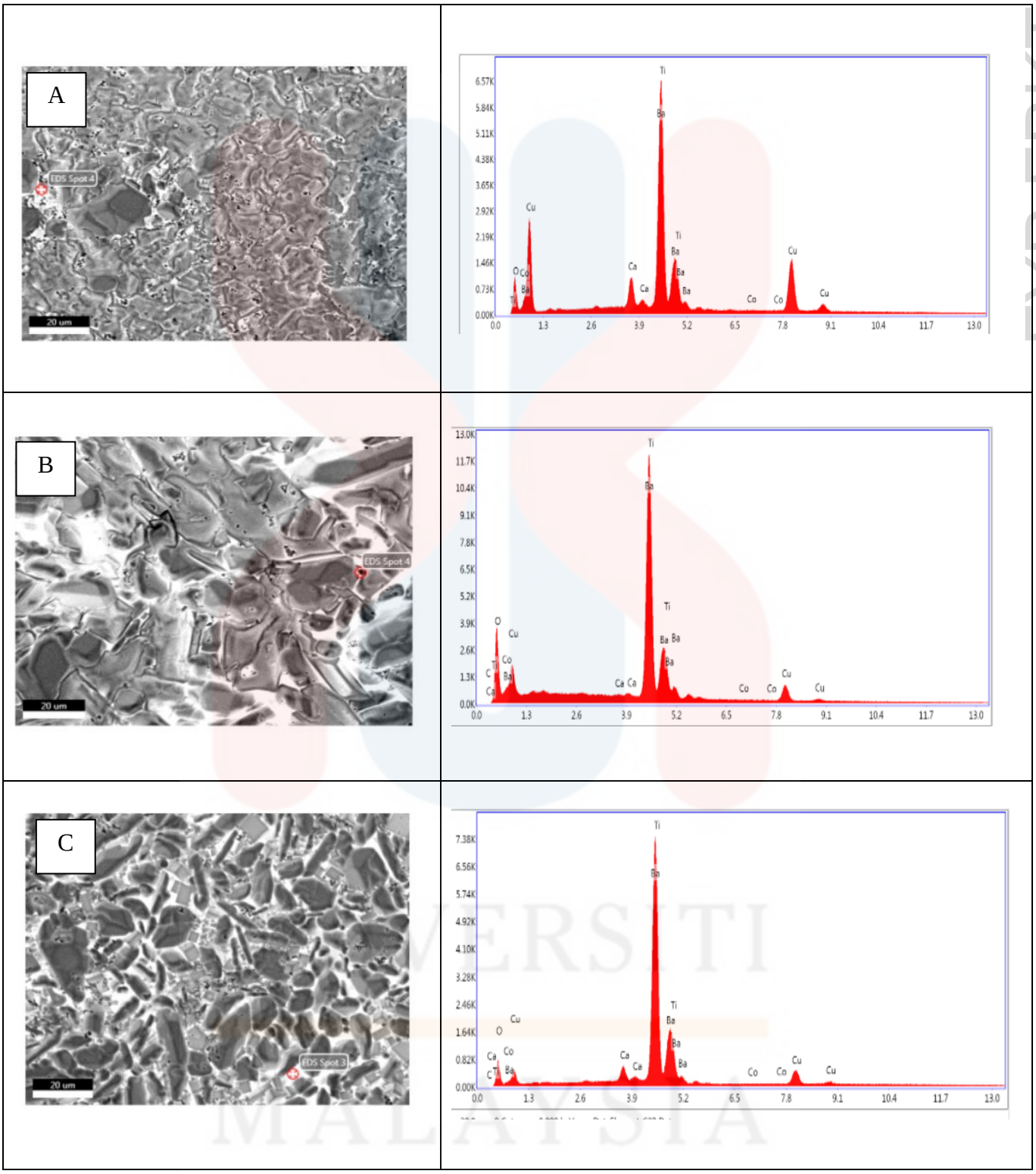

Figure 4.10: EDS analysis for CCTO/BT A)0.2mol% B)0.5mol% C)1.0mol%

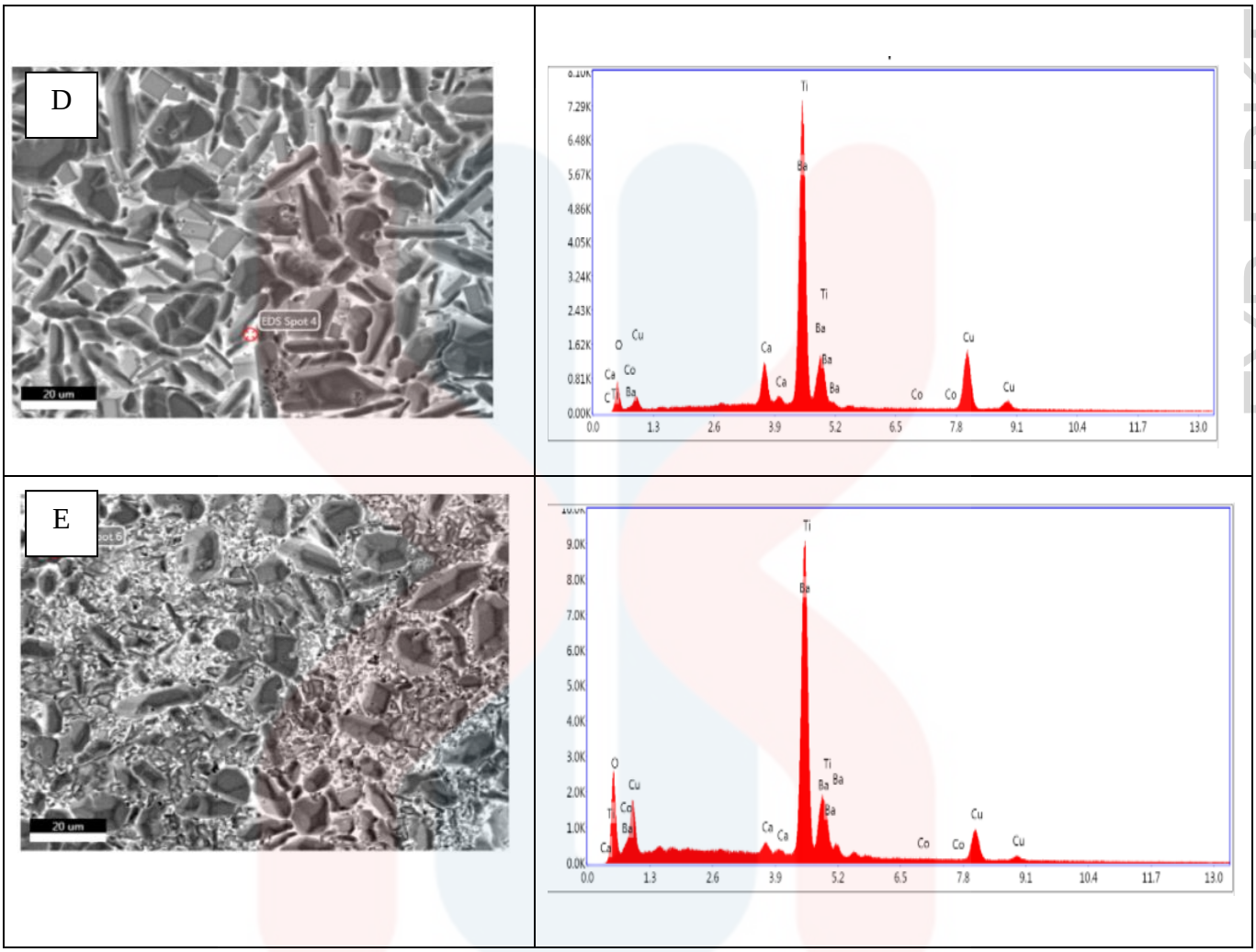

Figure 4.11: EDS analysis for CCTO/BT D)1.2mol% E)1.5mol%

4.4.4 Dielectric Properties

The dielectric constant and dielectric loss of different composition of CCTO/BT composite at frequency to 10 MHz and room temperature were conducted by using LCR Meter in Institute Nanoelectric and Electronic (INEE), University Malaysia Perlis (UniMAP), Perlis.

Figure 4.12 shown an increasing dielectric constant CCTO/BT content at 10 MHz between 7.54 and 50.5. Theoretically, as composition increases, space charge polarisation at the particle level will increase a material's dielectric properties(Karim et

al., 2017) and formation of large dipoles in the ceramic particle(Salaeh et al., 2011). It also shows the dielectric constant is gradually decreasing over the increasing of frequency testing. These phenomena happen due to the dielectric relaxation of ceramic particles (Salaeh et al., 2011) and poor interfacial polarisation or Maxwell-Wagner-Sillar effect which exist in heterogeneous dielectric materials(Li et al., 2023).

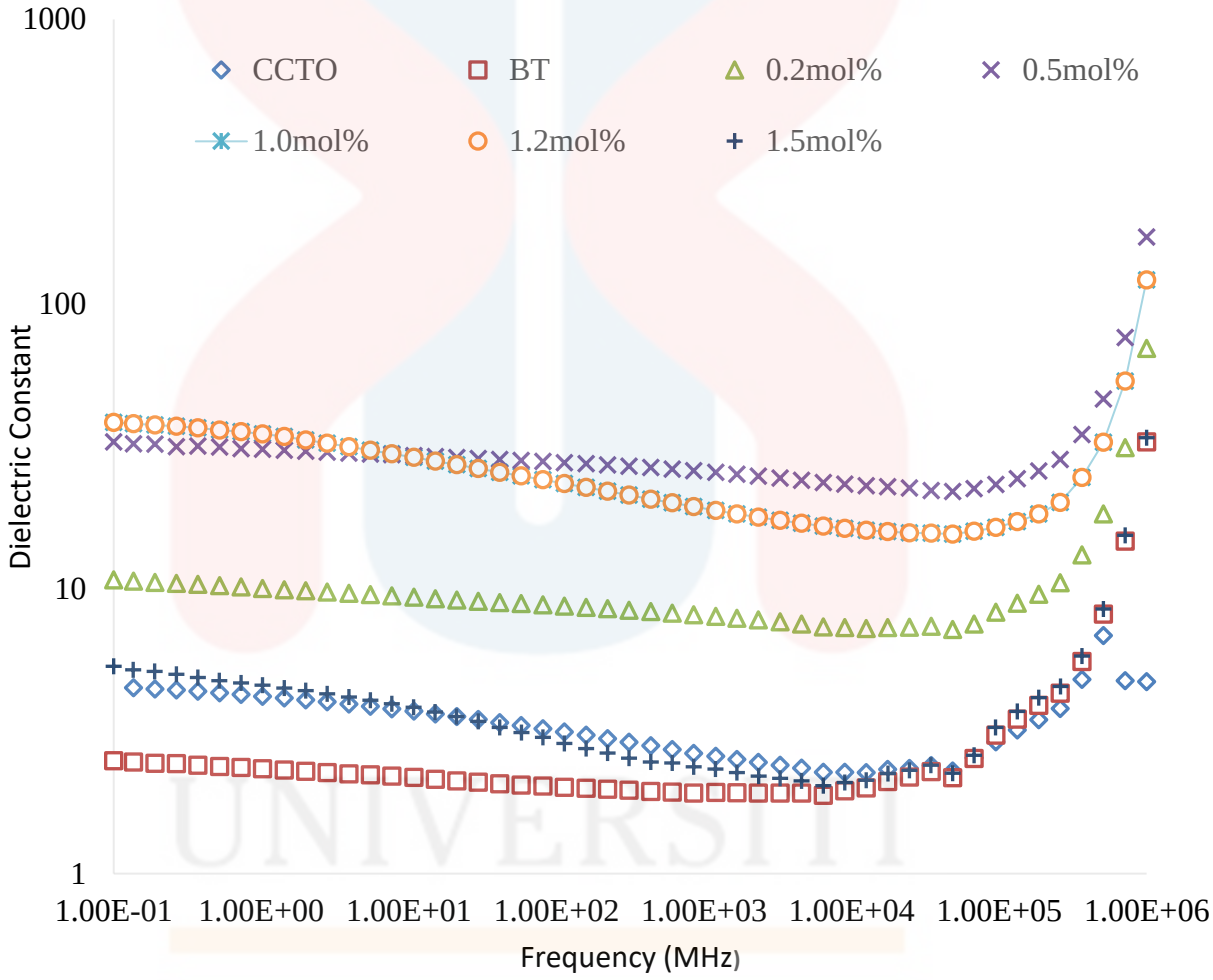

Figure 4.12: Dielectric constant of Composition between CCTO and BT

While the dielectric loss properties of CCTO/BT composite in Figure 4.13 show decrease from 6.1 to 1.0 at 10 MHz meanwhile the increasing frequency 11 to 31 MHz until the relaxation phenomenon occur. As suggested by (Karim et al., 2017), this

happen due to space charge polarisation which attributes to the lost effectiveness to catch up with a high frequency alternating electric field. Besides, the dielectric loss of the composite also shows decreasing along with increasing filler loading.

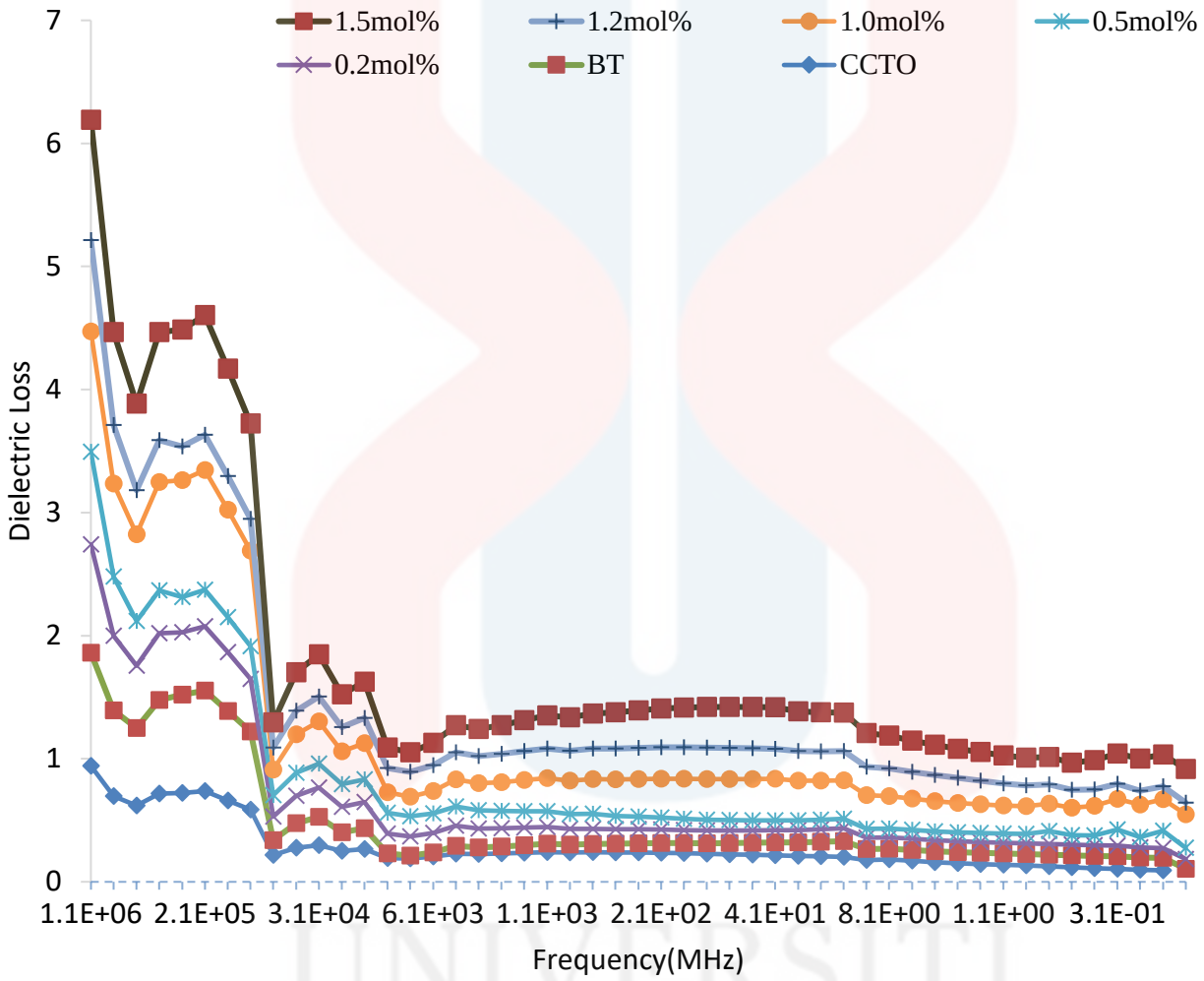

Figure 4.13: Dielectric loss of different composition CCTO/BT

CHAPTER 5

CONCLUSION AND RECOMMENDATION

CONCLUSION

In this study, BT and CCTO powder was chosen due to the well-known high dielectric properties. Combining the low loss of BT with the high dielectric constant of CCTO could maximise the advantages of both compounds. This study investigates the electrical and microstructural properties of BT and CCTO composites that were created using the solid-state reaction technique. The effect of composition between CCTO and BT was studied with few analysis such as XRD, TGA/DSC, Density and Porosity, Dielectric and SEM.

At the end of this study, CCTO and BT powder was successfully synthesised, and this can be observed through XRD analysis, 93.3wt% (CCTO) and 75.5wt% (BT) phase formed using solid-state reaction at calcination temperature of 900℃ for 12 hours and 1200℃ for 4hours. Then, CCTO mix with BT successfully fabricated at 0.2mol%,0.5mol%,1.0mol%,1.2mol% and 1.5mol%. Furthermore, in terms of porosity, 0.5mol% has the lowest porosity, while the density of CCTO/BT is 0.2mol% pallet at 4.2 g/cm^3 and the lowest is 1.2mol% pallet at 2.66g/cm^3. In additional, electrical properties, it shows an increasing CCTO/BT content can improve the dielectric constant from between 7.54 and 50.5 at 10 MHz and dielectric loss is decreasing from 6.1 to 1.0 at 10 MHz. In conclusion, all the testing that throughout, the most excellent composition that exhibits excellent properties is 1.2mol% of CCTO/BT.

RECOMMENDATION

A few suggestions would like to be made for additional study in the future. First, improve the milling time by using a high energy ball mill to add more defeat, which facilitates easier ion and electron migration during the calcination process. The dielectric properties of CCTO and BT powder can be enhanced using chemical reaction methods to produce nano size powder or nano size raw materials. In addition, to prevent errors, it is crucial to calibrate and verify the furnace's operating temperature. Then, a wider frequency range can be used to test the dielectric characteristics of the composition CCTO/BT.

REFERENCES

Ab Rahman, M. F., Hutagalung, S. D., Ahmad, Z. A., Ain, M. F., & Mohamed, J. J. (2015). The effect of different dopant site (Cu and Ca) by magnesium on CaCu3Ti4O12 dielectric properties. *Journal of Materials Science: Materials in Electronics*, *26*(6), 3947–3956. https://doi.org/10.1007/s10854-015-2929-z

Abdelal, O. A. A., Hassan, A. A., & Ali, M. E. (2012). Dielectric Properties of Calcium Copper Titanates (CaCu3Ti4O12) Synthesized by Solid State Reaction. *Arab Journal of Nuclear Science and Applications*, *45*(4), 354–361.

Ahmadipour, M., Ain, M. F., & Ahmad, Z. A. (2016). A Short Review on Copper Calcium Titanate (CCTO) Electroceramic: Synthesis, Dielectric Properties, Film Deposition, and Sensing Application. *Nano-Micro Letters*, *8*(4), 291–311. https://doi.org/10.1007/s40820-016-0089-1

Almeida, A. F. L., De Oliveira, R. S., Góes, J. C., Sasaki, J. M., Souza Filho, A. G., Mendes Filho, J., & Sombra, A. S. B. (2002). Structural properties of CaCu3Ti4O12 obtained by mechanical alloying. *Materials Science and Engineering B: Solid-State Materials for Advanced Technology*, *96*(3), 275–283. https://doi.org/10.1016/S0921-5107(02)00379-3

Biran, A., & López-Pulido, R. (2014). Basic Ship Hydrostatics. In *Ship Hydrostatics and Stability*. https://doi.org/10.1016/b978-0-08-098287-8.00002-5

Callister Jr, W. D., & Rethwisch, D. G. (2018). Characteristics, Application, and Processing of Polymers. In *Materials Science and Engineering - An Introduction*.

Country, E. (2013). Ceramics and Its Dimensions Ceramics and. *The Himalayan Physics*, *4*(4), 80–82.

Daou, R. A. Z. (2013). Resistors: Theory of operation, behavior and safety regulations. In *Resistors: Theory of Operation, Behavior and Safety Regulations*.

Du, J., Zhou, M. M., Ma, L. L., Cao, F., Xiao, J. J., Yu, Z. P., Qiu, X. L., & Wang, M. M. (2016). Preparation and characterization of high dielectric calcium copper titanate/polyimide composite films. *High Performance Polymers*, *28*(8), 908–914. https://doi.org/10.1177/0954008315609971

Egbo, M. K. (2021). A fundamental review on composite materials and some of their applications in biomedical engineering. *Journal of King Saud University - Engineering Sciences*, *33*(8), 557–568. https://doi.org/10.1016/j.jksues.2020.07.007

Glazer, A. M. (1972). The classification of tilted octahedra in perovskites. *Acta Crystallographica Section B Structural Crystallography and Crystal Chemistry*, *28*(11), 3384–3392. https://doi.org/10.1107/s0567740872007976

Haque, M. J., Mostari, M. S., Ankur, S. B. R., & Rahman, M. S. (2021). Enhanced dielectric, ferroelectric and optical properties of Ba (Zr0.15Ti0.85) O3 ceramics incorporated with MgO. *Results in Materials*, *10*(February), 100176. https://doi.org/10.1016/j.rinma.2021.100176

Jumpatam, J., Putasaeng, B., Yamwong, T., Thongbai, P., & Maensiri, S. (2014). A novel strategy to enhance dielectric performance and non-Ohmic properties in Ca2Cu2-xMgxTi4O12. *Journal of the European Ceramic Society*, *34*(12), 2941–2950. https://doi.org/10.1016/j.jeurceramsoc.2014.04.037

Karim, S. A., Sulaiman, M. A., Masri, M. N., Ahmad, Z. A., & Ain, M. F. (2017). The dielectric properties of CaCu3Ti4O12 at various calcination temperatures. *Materials Science Forum*, *888 MSF*, 117–120. https://doi.org/10.4028/www.scientific.net/MSF.888.117

Kumar, R. R., Sanodia, S., Jain, N., Kumar, R. R., Sundararajan, T., Prabu, S. B., & Vidyavathy, S. M. (2012). Combined effects of milling and calcination methods on the characteristics of nanocrystalline barium titanate. *Materials Research Bulletin*, *47*(6), 1448–1454. https://doi.org/10.1016/j.materresbull.2012.02.044

Li, T., Chen, J., Liu, D., Zhang, Z., Chen, Z., Li, Z., Cao, X., & Wang, B. (2014). Effect of NiO-doping on the microstructure and the dielectric properties of CaCu3Ti4O12 ceramics. *Ceramics International*, *40*(7 PART A), 9061–9067. https://doi.org/10.1016/j.ceramint.2014.01.119

Majhi, K., Prakash, B. S., & Varma, K. B. R. (2007). Extreme values of relative permittivity and dielectric relaxation in Sr2SbMnO6 ceramics. *Journal of Physics D: Applied Physics*, *40*(22), 7128–7135. https://doi.org/10.1088/0022-3727/40/22/040

More, S. P., & Topare, R. J. (2016). The review of various synthesis methods of barium titanate with the enhanced dielectric properties. *AIP Conference Proceedings*, *1728*(July 2016). https://doi.org/10.1063/1.4946611

Mu, C. H., Liu, P., He, Y., Zhou, J. P., & Zhang, H. W. (2009). An effective method to decrease dielectric loss of CaCu3Ti4O12 ceramics. *Journal of Alloys and Compounds*, *471*(1–2), 137–141. https://doi.org/10.1016/j.jallcom.2008.04.040

Negi, R. R., Chandrasekhar, M., & Kumar, P. (2019). Structural, microstructural, dielectric and ferroelectric properties of BaTiO3-based ceramics. *Processing and Application of Ceramics*, *13*(2), 164–172. https://doi.org/10.2298/PAC1902164N

Pant, H. C., Patra, M. K., Verma, A., Vadera, S. R., & Kumar, N. (2006). Study of the dielectric properties of barium titanate-polymer composites. *Acta Materialia*, *54*(12), 3163–3169. https://doi.org/10.1016/j.actamat.2006.02.031

Petrášek, J., Ctibor, P., Sedláček, J., & Lukáč, F. (2021). Synthesis and pressure-assisted sintering of cacu3ti4o12 dielectrics. *Ceramics*, *4*(3), 447–466. https://doi.org/10.3390/ceramics4030033

Rahman, M. F. A., Abu, M. J., Ain, M. F., Mohamed, J. J., & Ahmad, Z. A. (2016). Effect of Calcination Temperature on Dielectric Properties of CaCu3Ti4O12 Ceramics. *Procedia Chemistry*, *19*, 910–915. https://doi.org/10.1016/j.proche.2016.03.134

Salaeh, S., Muensit, N., Bomlai, P., & Nakason, C. (2011). Ceramic/natural rubber composites: Influence types of rubber and ceramic materials on curing, mechanical, morphological, and dielectric properties. *Journal of Materials Science*, *46*(6), 1723–1731. https://doi.org/10.1007/s10853-010-4990-6

Schmidt, R., Pandey, S., Fiorenza, P., & Sinclair, D. C. (2013). Non-stoichiometry in "caCu3Ti4O 12" (CCTO) ceramics. *RSC Advances*, *3*(34), 14580–14589. https://doi.org/10.1039/c3ra41319e

Subramanian, M. A., Li, D., Duan, N., Reisner, B. A., & Sleight, A. W. (2000). High dielectric constant in ACu3Ti4O12 and ACu3Ti3FeO12 phases. *Journal of Solid State Chemistry*, *151*(2), 323–325. https://doi.org/10.1006/jssc.2000.8703

Sulaiman, M. A., Hutagalung, S. D., Ain, M. F., & Ahmad, Z. A. (2010). Dielectric properties of Nb-doped CaCu3Ti4O12 electroceramics measured at high frequencies. *Journal of Alloys and Compounds*, *493*(1–2), 486–492. https://doi.org/10.1016/j.jallcom.2009.12.137

Tewatia, K., Sharma, A., Sharma, M., & Kumar, A. (2020). Factors affecting morphological and electrical properties of Barium Titanate: A brief review. *Materials Today: Proceedings*, *44*(xxxx), 4548–4556. https://doi.org/10.1016/j.matpr.2020.10.813

Wan, W., Luo, J., Huang, C. e., Yang, J., Feng, Y., Yuan, W. X., Ouyang, Y., Chen, D., & Qiu, T. (2018). Calcium copper titanate/polyurethane composite films with high dielectric constant, low dielectric loss and super flexibility. *Ceramics International*, *44*(5), 5086–5092. https://doi.org/10.1016/j.ceramint.2017.12.108

Yaseen, J. (2019a). *Preparation the Barium Titanate (Batio 3) Material and study the effect of Fast Neutrons , Gamma – Ray on Its Dielectric Properties and Microstructure*. *August 2018*, 6–10.

Zhang, J., Zheng, J., Liu, Y., Zhang, C., Hao, W., Lei, Z., & Tian, M. (2019). The dielectric properties of CCTO ceramics prepared via different quick quenching methods. *Materials Research Bulletin*, *115*, 49–54. https://doi.org/10.1016/j.materresbull.2019.03.006

APPENDICES

APPENDIX A

Calculation on starting materials needs to prepare 100gram of pure CCTO. The chemical reaction is shown as Equation A1. The molecular weight is shown below:

$CaCO_3 + 3CuO + 4TiO_2 \longrightarrow CaCu_3Ti_4O_{12} + CO_2$

Relative molecular weight.

$CaCO_3$ = 40.078 + 12.011+3(15.999) =100.086 g/mol

CuO= 63.546 +15.999 = 79.545 g/mol

TiO_2 = 47.867+2(15.999) = 79.866 g/mol

Mole of $CaCu_3Ti_4O_{12}$ = mass/ relative molecular mass

=100/ [40.078+3(63.546) +4(47.867) +12(15.999)]

=0.163 g/mol

Based on Equation 1, amount of CaCO3, CuO and TiO2 needed are:

$CaCO_3$=100.086 x 1x 0.163 = 16.3g

CuO= 79.545 x 3 x 0.163 = 38.9g

TiO_2=79.866 x 4 x 0.163 = 52.1g

Calculation on starting materials needs to prepare 100gram of pure BT. The chemical reaction is shown as Equation A1. The molecular weight is shown below:

$BaCO_3 + TiO_2 \longrightarrow BaTiO_3 + CO_2$

Relative molecular weight.

$BaCO_3$ = 137.33 + 12.011+3(15.999) = 197.338g/mol

TiO_2 = 47.867+2(15.999) = 79.866 g/mol

Mole of $BaTiO_3$ = mass/ relative molecular mass

=100/ [137.33+ 47.867+3(15.999)]

=0.429 g/mol

Based on Equation 1, amount of $BaCO_3$, and TiO_2 needed are:

$BaCO_3$=197.338 x 1 x 0.429 = 84.66g

TiO_2=79.866 x 1 x 0.429 = 34.26g

APPENDIX B

For composition,

x = 0, 0.2,0.5,1.0,1.2,1.5

x = 0, $BaTiO_3$ = 20g

x = 0.2, $BaTiO_3.xCaCu_3Ti_4O_{12}$

233.176 + (0.2) (614.174) = 356.01g/mol

13.1g + 6.9g = 20g

x = 0.5, $BaTiO_3.xCaCu_3Ti_4O_{12}$

233.176 + (0.5) (614.174) = 540.262g/mol

8.6g + 11.4g = 20g

x = 1.0, $BaTiO_3.xCaCu_3Ti_4O_{12}$

233.176 + (1.0) (614.174) = 847.348g/mol

5.5g + 14.5g = 20g

x = 1.2, $BaTiO_3.xCaCu_3Ti_4O_{12}$

233.176 + (1.2) (614.174) = 970.182g/mol

4.8g + 16.2g = 20g

x = 1.5, $BaTiO_3.xCaCu_3Ti_4O_{12}$

233.176 + (1.5) (614.174) = 1154.434g/mol

4.0g + 16.0g = 20g

APPENDIX C

XRD COD pattern

B1: CCTO powder

Pattern: COD 1532158 Radiation: 1.54060 Quality: Quality Unknown

Formula	CaCu3O12Ti4
Name	
Name (mineral)	
Name (common)	
Status	Status Unknown
Ambient	Yes

Lattice:	Cubic
S.G.:	I m -3 (204)
a =	7.40370
a/b =	1.00000
c/b =	1.00000
Z =	2
Mol. weight =	
Volume [CD] =	405.83
Dx =	
Dm =	
I/Icor =	6.590

Primary Reference
Subramanian M.A., Sleight A.W., "A Cu3 Ti4 O12 and A Cu3 Ru4 O12 perovskites: high dielectric constantsand valence degeneracy", Solid State Sciences 4 (2002) 347-351.

Wavelength :	1.54060
SS/FOM:	
Filter:	Not specified
d-spacing:	

d	2θ	I fix	h	k	l
5.23520	16.922	32	1	1	0
3.70180	24.021	6	2	0	0
3.02250	29.530	44	2	1	1
2.61760	34.228	1000	2	2	0
2.34130	38.417	67	3	1	0
2.13730	42.251	61	2	2	2
1.97870	45.821	38	3	2	1
1.85090	49.187	276	4	0	0
1.74510	52.387	15	4	1	1
1.65550	55.459	4	4	2	0
1.57850	58.418	9	3	2	3
1.51130	61.287	428	4	2	2
1.45200	64.080	6	5	0	1
1.35170	69.483	8	5	2	1
1.30880	72.109	103	4	4	0
1.26970	74.699	18	5	0	3
1.23390	77.259	11	6	0	0
1.20100	79.790	7	6	1	1
1.17060	82.301	114	6	2	0
1.14240	84.797	1	5	4	1
1.11610	87.287	1	6	2	2
1.09160	89.766	2	6	3	1
1.06860	92.249	30	4	4	4
1.04700	94.736	2	7	0	1
1.02670	97.227	4	6	4	0
1.00750	99.737	5	7	1	2

B2: BT powder

Pattern: COD 1507757 Radiation: 1.54060 Quality: Quality Unknown

Formula	BaO3Ti
Name	
Name (mineral)	
Name (common)	
Status	Status Unknown
Ambient	Yes

Lattice:	Cubic
S.G.:	P m -3 m (221)

Mol. weight =	
Volume [CD] =	64.35
Dx =	
Dm =	
I/Icor =	12.620

a =	4.00730		
a/b =	1.00000	Z =	1
c/b =	1.00000		

Primary Reference
Natheer B. Mahmood, Emad K. Al-Shakarchi, "Three Techniques Used to Produce BaTiO3 Fine Powder", Journal of Modern Physics 2 (2011) 1420-1428.

Wavelength :	1.54060
SS/FOM:	
Filter:	Not specified
d-spacing:	

d	2θ	I fix	h	k	l
4.00730	22.165	195	1	0	0
2.83360	31.548	999	1	0	1
2.31360	38.895	245	1	1	1
2.00360	45.220	326	2	0	0
1.79210	50.914	91	2	0	1
1.63600	56.178	337	2	1	1
1.41680	65.870	168	2	0	2
1.33580	70.432	43	3	0	0
1.26720	74.872	127	3	0	1
1.20820	79.220	63	3	1	1
1.15680	83.501	50	2	2	2
1.11140	87.750	19	2	3	0
1.07100	91.983	143	3	2	1